USAARL-TECH-FR--2021-06

Increasing Survival Rate Following Hemorrhagic Shock and Traumatic Brain Injury in Austere Environments - Transport Data Analysis

Amy Lloyd, Rachel Kinsler, Laura Kroening, Andrew Meyer,
Andrew Dodd, Julie Rannou-Latella, Rebecca Dodd,
Megan Vermillion, & Jeff Molles

Notice

Qualified Requesters

Qualified requesters may obtain copies from the Defense Technical Information Center (DTIC), Cameron Station, Alexandria, Virginia 22314. Orders will be expedited if placed through the librarian or other person designated to request documents from DTIC.

Change of Address

Organizations receiving reports from the U.S. Army Aeromedical Research Laboratory on automatic mailing lists should confirm correct address when corresponding about laboratory reports.

Disposition

Destroy this document when it is no longer needed. Do not return it to the originator.

Disclaimer

The views, opinions, and/or findings contained in this report are those of the author(s) and should not be construed as an official Department of the Army position, policy, or decision, unless so designated by other official documentation. Citation of trade names in this report does not constitute an official Department of the Army endorsement or approval of the use of such commercial items.

Animal Use

The animal research reported herein was conducted in compliance with the Department of Defense Instruction 3216.01 (September 13, 2010) and referenced federal statutes; the Animal Welfare Act/Regulations and the PHS Policy on Human Care and Use of Laboratory Animals/Guide for Care and Use of Laboratory Animals.

REPORT DOCUMENTATION PAGE

Form Approved
OMB No. 0704-0188

PLEASE DO NOT RETURN YOUR FORM TO THE ABOVE ADDRESS.

1. REPORT DATE *(DD-MM-YYYY)*	2. REPORT TYPE	3. DATES COVERED *(From - To)*
11-12-2020	Final Report	1Oct2018 - 30Sep2020

4. TITLE AND SUBTITLE

Increasing Survival Rate Following Hemorrhagic Shock and Traumatic Brain Injury in Austere Environments – Transport Data Analysis

5a. CONTRACT NUMBER

N/A

5b. GRANT NUMBER

N/A

5c. PROGRAM ELEMENT NUMBER

6.2

6. AUTHOR(S)

A. Lloyd[1,2], R. Kinsler[1], L. Kroening[1,2], A. Mayer[3,4], A. Dodd[3], J. Rannou-Latella[3], R. Dodd[3], M. Vermillion[3], & J. Molles[1,2]

5d. PROJECT NUMBER

W81XWH-16-DMRDP-CCCRP-PFCRA

5e. TASK NUMBER

N/A

5f. WORK UNIT NUMBER

N/A

7. PERFORMING ORGANIZATION NAME(S) AND ADDRESS(ES)

U.S. Army Aeromedical Research Laboratory
P.O. Box 620577
Fort Rucker, AL 36362

8. PERFORMING ORGANIZATION REPORT NUMBER

USAARL-TECH-FR--2021-06

9. SPONSORING/MONITORING AGENCY NAME(S) AND ADDRESS(ES)

Congressionally Directed Medical Research Programs
1077 Patchel Street
Fort Detrick, MD 21702-5024

10. SPONSOR/MONITOR'S ACRONYM(S)

CDMRP

11. SPONSOR/MONITOR'S REPORT NUMBER(S)

12. DISTRIBUTION/AVAILABILITY STATEMENT

Approved for public release; distribution unlimited.

13. SUPPLEMENTARY NOTES

[1]U.S. Army Aeromedical Research Laboratory; [2]Goldbelt Frontier, LLC; [3]The Mind Research Network/Lovelace Biomedical Research Institute; [4]University of New Mexico School of Medicine

14. ABSTRACT

There were five cohorts of animals tested during the Prolonged Field Care project. There were 28 non-transport animals and 26 transport animals in total from the five cohorts. The non-transport animals were loaded onto a M997 ambulance lower left litter berth, but the vehicle was stationary. The transport animals were transported on a track for a total of about 40 minutes. There were two sets of track passes, each set of track passes contained two bumpy tracks (inside and outside bumpy), two smooth tracks (inside and outside smooth), and a half straddle between one of the bumpy tracks and one of the smooth tracks. At the very end of each set of track passes the vehicle went over an embedded six inch steel pipe, known as the half round, which created a significant mechanical shock. There were five six-degree of freedom sensors used during testing. Three where placed on the animal (head, scapula, and pelvis), one was placed underneath the back board, and one was placed on the litter berth. For the data, the Root Mean Square (RMS), Power Spectral Density (PSD), and Fast Fourier Transform (FFT) was calculated. From the RMS analysis of the data, the pelvis showed the most movement for each of the different tracks. For all of the tracks, the RMS of the pelvis was 12 to 16% higher than the average RMS of the track. The vehicle had the lowest RMS on each of the tracks, 9 to 16% lower than the average RMS. The PSD analysis showed the most energy, in the 2 to 3 Hz range for all of the tracks, and this was also seen in the FFT analysis.

15. SUBJECT TERMS

Traumatic brain injury, Hemorrhagic shock, Rough ground transport, Vibration, Dynamic head acceleration, Mechanical shock, Animal, Blood loss, Head trauma, Swine, Transmissibility, Root mean square, Power spectral density, Fourier transform

16. SECURITY CLASSIFICATION OF:			17. LIMITATION OF ABSTRACT	18. NUMBER OF PAGES	19a. NAME OF RESPONSIBLE PERSON
a. REPORT	b. ABSTRACT	c. THIS PAGE			Loraine St. Onge, PhD
UNCLAS	UNCLAS	UNCLAS	SAR	37	19b. TELEPHONE NUMBER *(Include area code)* 334-255-6906

This page is intentionally blank.

Acknowledgements

The authors would like to express sincere gratitude to the following people and organizations for their valuable contributions to this research project:

- The United States Army Reserve for providing a vehicle for testing. Specifically SGT Carlos Domenech at the New Mexico Army Reserve, for his help in securing the vehicle for testing.
- New Mexico Army National Guard for providing vehicles for testing.
- The Defense Health Program for providing funding for this project.

This page is intentionally blank.

Table of Contents

List of Figures

Table of Contents (continued)

List of Tables

Introduction

The use of improvised explosive devices in the conflicts in Iraq and Afghanistan has resulted in a wide range of injuries, few of which have attracted more public attention than traumatic brain injury (TBI) and hemorrhagic shock (HS). TBI has been referred to by physicians and neuroscientists studying the phenomenon as the signature injury of Operation Iraqi Freedom and Operation Enduring Freedom. Blast has been implicated in upwards of 70% of all traumas, with rapid accelerative and decelerative force from tertiary blast injury often resulting in TBI. Similarly, approximately 90% of all preventable mortalities involve HS (Mayer, A., 2019). The goal of this study is to carefully model the effects of medical transport on such patients after a realistic rotational acceleration head injury and subsequent HS. The information gathered from this study may have tremendous potential to aid not only military healthcare providers, but the civilian medical community as well. Head trauma and severe blood loss are exceedingly common (e.g., sports injuries, motor vehicle accidents, falls) worldwide.

To examine this issue, a collaboration between the U.S. Army Aeromedical Research Laboratory (USAARL), Mind Research Network, and Lovelace Biomedical Research Institute (LBRI) was formed. A ride-quality course was designed based on data collected from military ground evacuation vehicles in the field, and built in collaboration with Aberdeen Test Center on the LBRI South campus. The vibrational data from transporting injured animal models or healthy human subjects on the track on the LBRI campus can be analyzed to characterize the transportation of the subject. A collaboration was formed separately with the New Mexico Army National Guard and United States Army Reserve was formed to obtain High Mobility Multipurpose Wheeled Vehicles for use as the ground ambulance for transport. USAARL was responsible for the transportation of the animals, which included securing the animal on the litter and instrumentation of the animal.

The overall objective of this paper is to characterize the vibrational data collected from the injured swine that were transported during the study. For this particular study, completed at LBRI, a polytrauma TBI and HS injured animal model was used to determine whether a novel drug therapy, EE-3-SO_4, prolongs survival time in an austere environment relative to sham. The TBI was initiated via a pneumatic device, HYGE™, (Cullen et al., 2016). For the TBI exposure, all animals were placed in ventral recumbency (sternal) in sphynx position. The animals' heads were secured with metal straps to the linkage assembly of the HYGE device through a custom-made bite bar that converts linear to angular (rotational) motion. The targeted angular peak velocity was 250 radians/second (s) in the coronal plane. Following the TBI exposure, animals were placed in lateral recumbency and subjected to arterial hemorrhage via controlled removal of approximately 40% of estimated total blood volume (Mayer et al., 2019; Mayer et al., 2020). After the polytrauma was completed the animals were either given an estrogen derivative drug EE-3-SO_4 or a placebo. To replicate an austere environment, the animals either underwent a rough ground transport on the track or remained stationary three hours after the blood loss procedure.

This technical report provides results from analyses of the transport data collected under the Defense Health Program Prolonged Field Care Research Award #W81XWH-16-DMRDP-

CCCRP-PFCRA, “Increasing Survival Rate Following Hemorrhagic Shock and Traumatic Brain Injury in Austere Environments.”

Test Methods

There were five cohorts of porcine animals tested during this project. The first in April 2019, the second in July 2019, the third in September 2019, the fourth in December 2019, and the fifth in February 2020. Each animal was given a TBI via an accelerative device and HS was created by removing approximately 40% of the estimated blood volume. After the blood loss procedure, the animals were monitored (without interventions) for three hours to simulate a prolonged field care (PFC) scenario until the transport phase of the experiment. The animals tested in the cohorts were either transport or non-transport. The transport animals were loaded onto a M997 U.S. Army ground ambulance into the lower left litter berth, secured, and taken on two sets of track passes, defined in Table 1. The total travel time for the transport animals was 40 minutes (min). This included 5 min for the transport to the track, 30 min for the track passes (15 min each), and 5 min for the transport from the track. The non-transport animals were loaded into the ground ambulance in the lower left litter berth, but the vehicle remained stationary. They were unloaded 40 min later; which simulated the total time that the transport animals would be in the vehicle.

Table 1. Test Conditions Experienced

	First Track Pass Set	**Second Track Pass Set**
Lap 1	Inside Bumpy	Inside Bumpy
Lap 2	Inside Smooth	Inside Smooth
Lap 3	Outside Bumpy	Outside Bumpy
Lap 4	Outside Smooth	Outside Smooth
Lap 5	Outside Half Straddle with Half Round	Inside Half Straddle with Half Round

Figure 1 describes the layout of the track as well as the sequence and direction of travel. The vehicle entered the track as shown in the lower left corner of the figure, and stopped at the beginning of the gravel straight away, and the first set of passes began. For each lap in the set of passes, there was a condition that changed. The vehicle started on the gravel section at 20 miles per hour (mph) (bottom of Figure 1), turned the corner, and then reached the track sections described in Table 1. The vehicle drove at 5 mph on each of the track sections, and completed the Half Round at 10 mph. The bumpy tracks refer to non-periodic bumps on the road meant to simulate an approximately 2 inch root mean square (RMS) average ride roughness. Straddle indicates the tires on one side of the vehicle are on one track section and the other tires are on another track section at the same time (either straddling both bumpy sections or one bumpy section and the smooth shoulder beside the bumpy track sections). The Half Round is a steel pipe embedded in the concrete, with a six inch rise, that created a significant mechanical shock when driven over.

This space is intentionally blank.

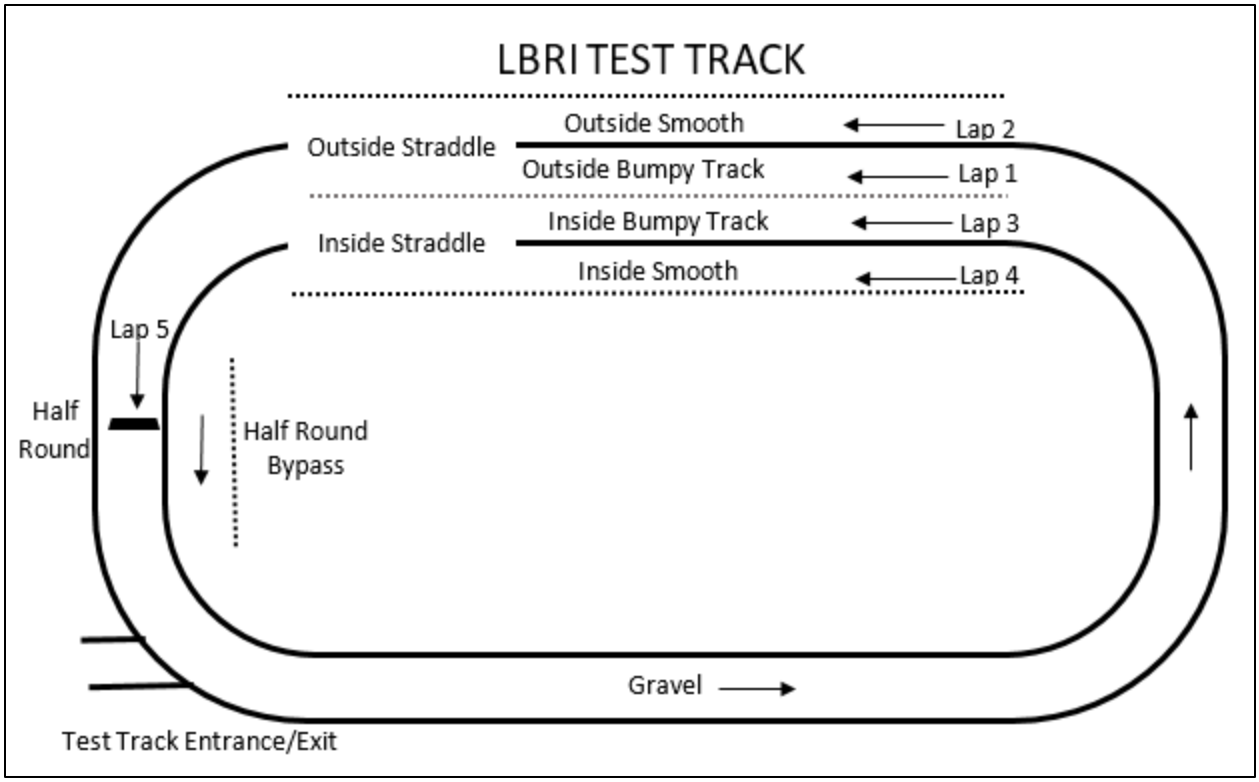

Figure 1. Test track with order and direction of travel.

The first four conditions are the same for both sets of track passes. For each of the first four conditions the Half Round was avoided by going around the obstacle on the inside. An example of the Inside Bumpy section can be seen in Figure 2, and the Inside Smooth section can be seen in Figure 3. The fifth condition for the track passes was a straddle. In the first set of passes the Outside Half Straddle was completed, so the left half of the vehicle was on the Outside Bumpy section and the right side of the vehicle was on the Outside Smooth section (as seen in Figure 4). For the second set of passes, the Inside Half Straddle was completed; the right side of the vehicle was on the Inside Smooth section and the left side of the vehicle was on the Inside Bumpy section. At the end of each straddle the Half Round was completed.

This space is intentionally blank.

Figure 2. Vehicle passing on Inside Bumpy section.

Figure 3. Vehicle passing on Inside Smooth section.

Figure 4. Vehicle passing on Outside Half Straddle section.

There were 26 transport animals and 28 non-transport animals in total from the five cohorts. Five 6 Degrees of Freedom (6DOF) sensors where used during testing. Three were placed on the animal, one was placed underneath the backboard, and one was placed on the litter berth. Figure 5 shows the sensor placement on the animal. The sensors on the backboard and litter berth were placed approximately underneath the animal's center of gravity. The sensor information was recorded using CoCo-90 data acquisition (DAQ) devices, manufactured by Crystal Instruments.

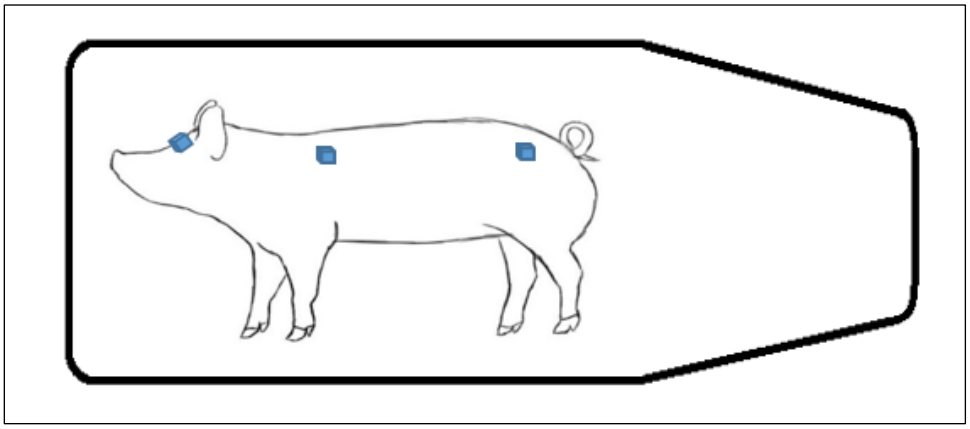

Figure 5. Animal sensor locations.

The sensors placed on the vehicle, backboard, and animal subject measured vibration acceleration in three main axes (*x*-axis, vehicle front-to-back; *y*-axis, vehicle side-to-side; and *z*-axis, ground-to-sky). Figure 6 shows the sensor placement on the back of the backboard and on the vehicle litter berth.

This space is intentionally blank.

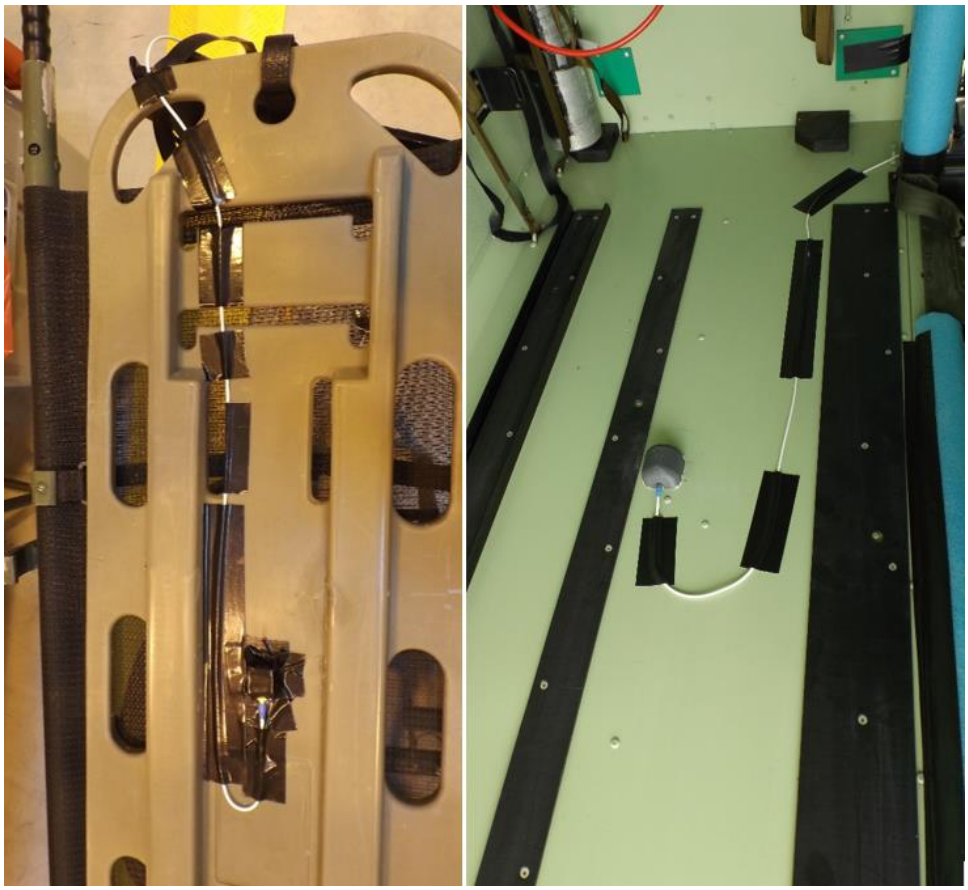

Figure 6. Board and vehicle sensor locations.

The DAQ devices collected data in separate channels for each axis of each sensor. Each DAQ device had 16 channels available. The first 15 channels of the DAQ device were used to collect data, and the 16th channel on each device was used to record a common square wave so the data could be synchronized between the two DAQ devices. The sensor connections are shown in Table 2. The same sensors were used in all five cohorts, but there were several different DAQ devices used during the testing. The pelvis sensor was split between the two DAQ devices, the accelerometer channels were connected to CoCo-90 #1, and the gyroscope channels were connected to CoCo-90 #2. This was done so that all five 6DOF sensors could be used.

This space is intentionally blank.

Table 2. Instrumentation Notes

CoCo-90	Sensor Location	Sensor Type	Channel	Axis	Sensitivity	Range
CoCo-90 #1	Animal's Brow Ridge (S/N: 163)	6DOF (Combined Accelerometers and Gyroscopes)	1	AX	209.390 millivolt per unit of gravity (mV/g)	±6 unit of gravity (g)
			2	AY	207.723 mV/g	±6 g
			3	AZ	208.539 mV/g	±6 g
			4	GX	0.9863 millivolt per degree per s (mV/deg/s)	±1000 degree per s (deg/s)
			5	GY	1.0225 mV/deg/s	±1000 deg/s
			6	GZ	1.0513 mV/deg/s	±1000 deg/s
	Animal's Scapula (S/N: 164)	6DOF	7	AX	211.755 mV/g	±6 g
			8	AY	198.013 mV/g	±6 g
			9	AZ	205.533 mV/g	±6 g
			10	GX	0.9415 mV/deg/s	±1000 deg/s
			11	GY	1.0125 mV/deg/s	±1000 deg/s
			12	GZ	1.0753 mV/deg/s	±1000 deg/s
	Animal's Pelvis (S/N: 166)	6DOF (Accelerometers)	13	AX	212.146 mV/g	±6 g
			14	AY	211.186 mV/g	±6 g
			15	AZ	208.596 mV/g	±6 g
	Synchronization Pulse (Square Wave CoCo-90 Output)	N/A	16	N/A	1000 mV/V	N/A
CoCo-90 #2	Center of Litter Berth (S/N: 315)	6DOF	1	AX	216.430 mV/g	±6 g
			2	AY	205.880 mV/g	±6 g
			3	AZ	201.780 mV/g	±6 g
			4	GX	1.033 mV/deg/s	±1000 deg/s
			5	GY	1.082 mV/deg/s	±1000 deg/s
			6	GZ	1.072 mV/deg/s	±1000 deg/s
	Center of Backboard (S/N: 167)	6DOF	7	AX	210.130 mV/g	±6 g
			8	AY	215.170 mV/g	±6 g
			9	AZ	208.230 mV/g	±6 g
			10	GX	1.0257 mV/deg/s	±1000 deg/s
			11	GY	0.9955 mV/deg/s	±1000 deg/s
			12	GZ	0.9919 mV/deg/s	±1000 deg/s
	Animal's Pelvis (S/N: 166)	6DOF (Gyroscopes)	13	GX	1.0225 mV/deg/s	±1000 deg/s
			14	GY	1.0381 mV/deg/s	±1000 deg/s
			15	GZ	0.9918 mV/deg/s	±1000 deg/s
	Synchronization Pulse (Square Wave CoCo-90 Output)	N/A	16	N/A	1000 mV/V	N/A

N/A = Not Applicable

In the first cohort, there were six transport animals and six non-transport animals, as shown in Table 3. Two animals did not survive the PFC phase. These animals are not classified as transport or non-transport because that phase was not reached.

Table 3. First Cohort Animal List (April 2019)

Date	Animal ID	Transport Condition	Notes
4/15/2019	7535	Did Not Survive PFC	N/A
4/16/2019	7528	Non-Transport	N/A
4/16/2019	7516	Transport	N/A
4/17/2019	7532	Transport	N/A
4/18/2019	7523	Non-Transport	N/A
4/18/2019	7536	Did Not Survive PFC	N/A
4/19/2019	7533	Non-Transport	N/A
4/22/2019	7530	Transport	N/A
4/23/2019	7522	Transport	N/A
4/23/2019	7521	Non-Transport	N/A
4/24/2019	7519	Transport	N/A
4/24/2019	7537	Non-Transport	N/A
4/25/2019	7538	Transport	N/A
4/25/2019	7518	Non-Transport	N/A

N/A = Not Applicable; PFC = Prolonged Field Care

In the second cohort, there were six non-transport animals and three transport animals. There were five animals that did not survive the PFC phase to get to the transport phase (Table 4). One of the animals (Animal ID 7663) survived the transport to the track but then deteriorated and had be transported back from the track immediately.

This space is intentionally blank.

Table 4. Second Cohort Animal List (July 2019)

Date	Animal ID	Transport Condition	Notes
7/8/2019	8144	Non-Transport	N/A
7/9/2019	8132	Non-Transport	N/A
7/9/2019	7706	Did Not Survive PFC	N/A
7/10/2019	8483	Did Not Survive PFC	N/A
7/10/2019	7696	Did Not Survive PFC	N/A
7/11/2019	8482	Transport	N/A
7/11/2019	8139	Transport	N/A
7/12/2019	7695	Non-Transport	N/A
7/15/2019	7698	Did Not Survive PFC	N/A
7/16/2019	7656	Transport	N/A
7/16/2019	7701	Did Not Survive PFC	N/A
7/17/2019	8484	Non-Transport	N/A
7/17/2019	7663	Transport	Animal only survived for the transport to and from the track.
7/18/2019	8142	Non-Transport	N/A

N/A = Not Applicable; PFC = Prolonged Field Care

There were five non-transport animals and six transport animals in the third cohort (Table 5). Two animals did not survive the PFC phase.

Table 5. Third Cohort Animal List (September 2019)

Date	Animal ID	Transport Condition	Notes
9/3/2019	8224	Non-Transport	N/A
9/4/2019	7983	Transport	N/A
9/4/2019	8249	Transport	N/A
9/5/2019	8235	Did Not Survive PFC	N/A
9/6/2019	8225	Non-Transport	N/A
9/6/2019	8190	Non-Transport	N/A
9/9/2019	8219	Transport	N/A
9/9/2019	8203	Did Not Survive PFC	N/A
9/10/2019	8242	Non-Transport	N/A
9/10/2019	8240	Transport	N/A
9/11/2019	8198	Non-Transport	N/A
9/11/2019	8246	Transport	N/A
9/12/2019	8222	Transport	N/A

N/A = Not Applicable; PFC = Prolonged Field Care

There were five non-transport animals and six transport animals in the fourth cohort (Table 6). Two animals did not survive the PFC phase of the testing. For one of the transport

animals (Animal ID 9180), the Inside Half Straddle data was not collected. During testing one of the DAQ devices turned off due to overheating and the set of laps had to be restarted. Due to the time restrictions on the transport, the IST was skipped.

Table 6. Fourth Cohort Animal List (December 2019)

Date	Animal ID	Transport Condition	Notes
12/2/2019	9172	Non-Transport	N/A
12/3/2019	9117	Did Not Survive PFC	N/A
12/3/2019	9119	Non-Transport	N/A
12/4/2019	9140	Transport	N/A
12/5/2019	9046	Transport	N/A
12/5/2019	9142	Non-Transport	N/A
12/6/2019	9204	Non-Transport	N/A
12/6/2019	9185	Non-Transport	N/A
12/9/2019	8843	Transport	N/A
12/9/2019	9177	Did Not Survive PFC	N/A
12/10/2019	9139	Transport	N/A
12/10/2019	9180	Transport	Missing Inside Half Straddle data.
12/11/2019	9181	Transport	N/A

N/A = Not Applicable; PFC = Prolonged Field Care

There were six non-transport animals and five transport animals in the third cohort (Table 7). Two animals did not survive the PFC phase until the transport phase of the testing. For the transport animals, the *y*-axis of the vehicle sensor was corrupted and unusable.

Table 7. Fifth Cohort Animal List (February 2020)

Date	Animal ID	Transport Condition	Notes
2/3/2020	9631	Non-Transport	N/A
2/4/2020	9630	Non-Transport	N/A
2/4/2020	9619	Did Not Survive PFC	N/A
2/5/2020	9646	Transport	Corrupted vehicle *y*-axis data
2/5/2020	9806	Non-Transport	N/A
2/6/2020	9628	Transport	Corrupted vehicle *y*-axis data
2/6/2020	9797	Did Not Survive PFC	N/A
2/7/2020	9620	Transport	Corrupted vehicle *y*-axis data
2/7/2020	9625	Non-Transport	N/A
2/10/2020	9650	Transport	Corrupted vehicle *y*-axis data
2/10/2020	9805	Non-Transport	N/A
2/11/2020	9804	Transport	Corrupted vehicle *y*-axis data
2/11/2020	9770	Non-Transport	N/A

N/A = Not Applicable; PFC = Prolonged Field Care

The data were first broken up into segments based on the individual track passes. Figure 7 shows what a pass of data looks like before it is segmented. The data segments are labeled underneath the graph. To allow for quicker data analysis, 10,000 data points (20 seconds [s]) of data for each track segment were sampled. Only 3,000 data points (6 s) were taken for the Half Round track segment because the event occurs so quickly. Figure 8 shows the segmented data for Figure 7. For Figure 8, the *y*-axis of the Outside Smooth and Inside Smooth graphs are smaller than the other track segments because the amplitudes for those tracks are much smaller.

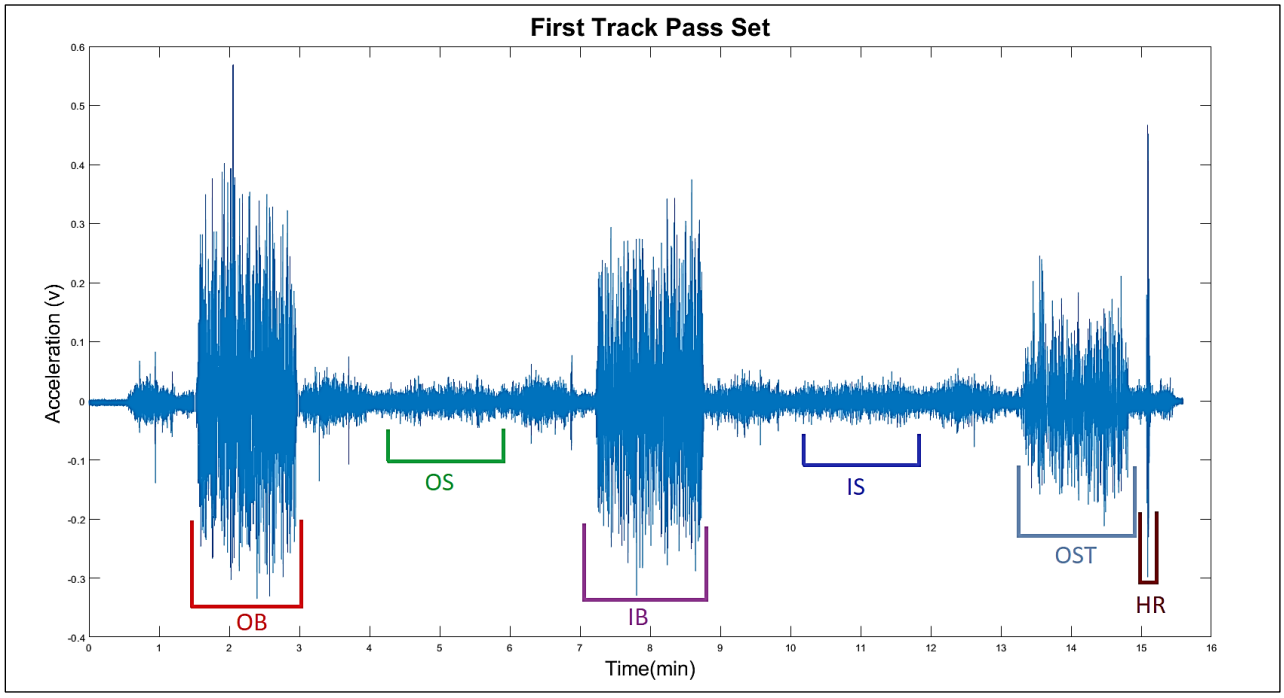

OB = Outside Bumpy, IB = Inside Bumpy, OS = Outside Smooth, IS = Inside Smooth,
OST = Outside Half Straddle, IST = Inside Half Straddle, HR = Half Round

Figure 7. Raw data example for first track pass set.

This space is intentionally blank.

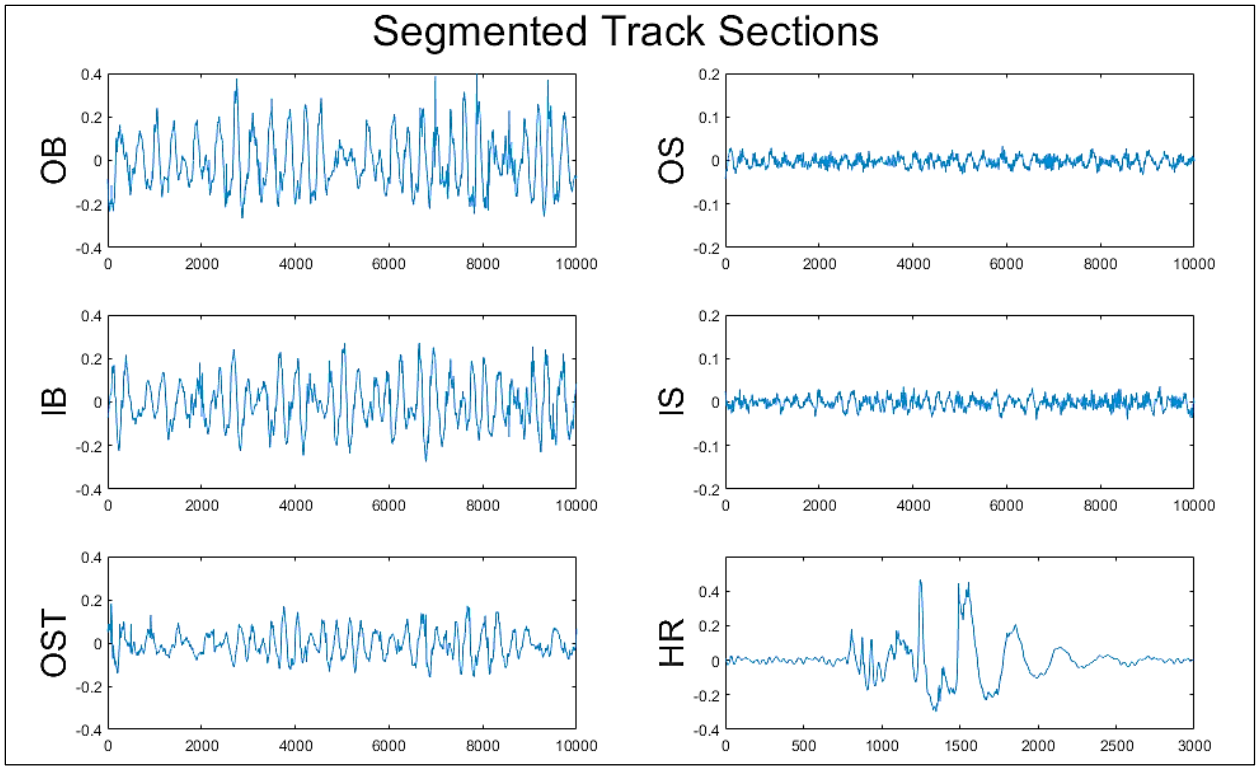

OB = Outside Bumpy, IB = Inside Bumpy, OS = Outside Smooth, IS = Inside Smooth,
OST = Outside Half Straddle, IST = Inside Half Straddle, HR = Half Round

Figure 8. Segmented data example for first track pass set.

Results

The data were analyzed using MATLAB® software. Before analyzing the data, a fourth-order Butterworth band pass filter was used on the data. The sampling rate was 500 Hertz (Hz). The bounds for the filter stop and pass frequencies were Fstop1 = 0.2 Hz, Fpass1 = 2.5 Hz, Fpass2 = 100 Hz, and Fstop2 = 240 Hz, shown in Figure 9. The RMS, Power Spectral Density (PSD), Fast Fourier Transform (FFT), and transmissibility were calculated after filtering the data.

This space is intentionally blank.

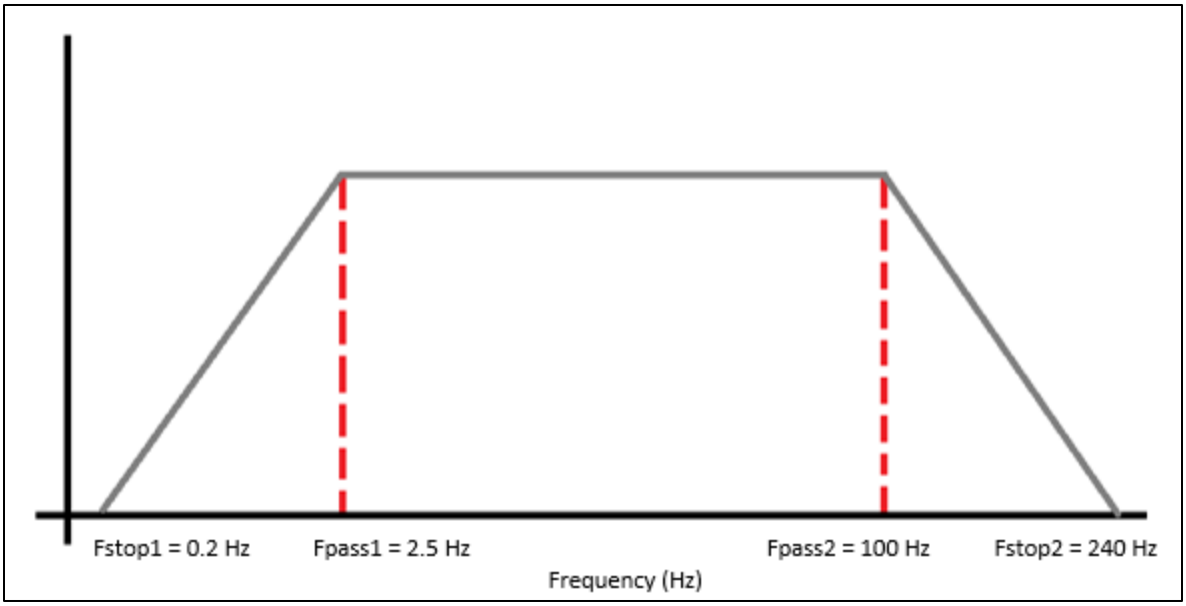

Figure 9. Fourth-order Butterworth band pass filter.

Root Mean Square

One way to determine the amount of vibrational energy present in a signal is to calculate the RMS of the acceleration values over a particular period of time. RMS acceleration is the square root of the sum of each acceleration value squared, divided by the total number of values. This allows the averages of amplitudes to be calculated. If a signed average was calculated the negative values would cancel out the positive values. The equation for this calculation is shown in Figure 10.

$$RMS = \sqrt{\frac{1}{N}\sum_{i=1}^{N} x(i)^2}$$

Figure 10. RMS equation.

The resultant RMS, or average of the three axes (*x*-, *y*- and *z*- axes), was also computed and the equation for this calculation is shown in Figure 11.

$$RMS = \sqrt{\frac{\sum_{i=1}^{N} x(i)^2 + y(i)^2 + z(i)^2}{N}}$$

Figure 11. Resultant RMS equation.

Figure 12 shows the average resultant RMS values for each sensor as shown by the different bar colors. The *x*-axis of the graph shows the track segments, and the black bars represent the standard deviations. For each of the track segments the resultant RMS for the animal's pelvis is 12 to 16% higher than the average RMS for all the other sensors. The sensor on the vehicle's litter berth (identified in the figure as "Vehicle") recorded the lowest RMS on each of the tracks, 9 to 16 % lower than the average RMS of the other sensors. The Outside Smooth and Inside Smooth tracks had the lowest standard deviation of the tracks.

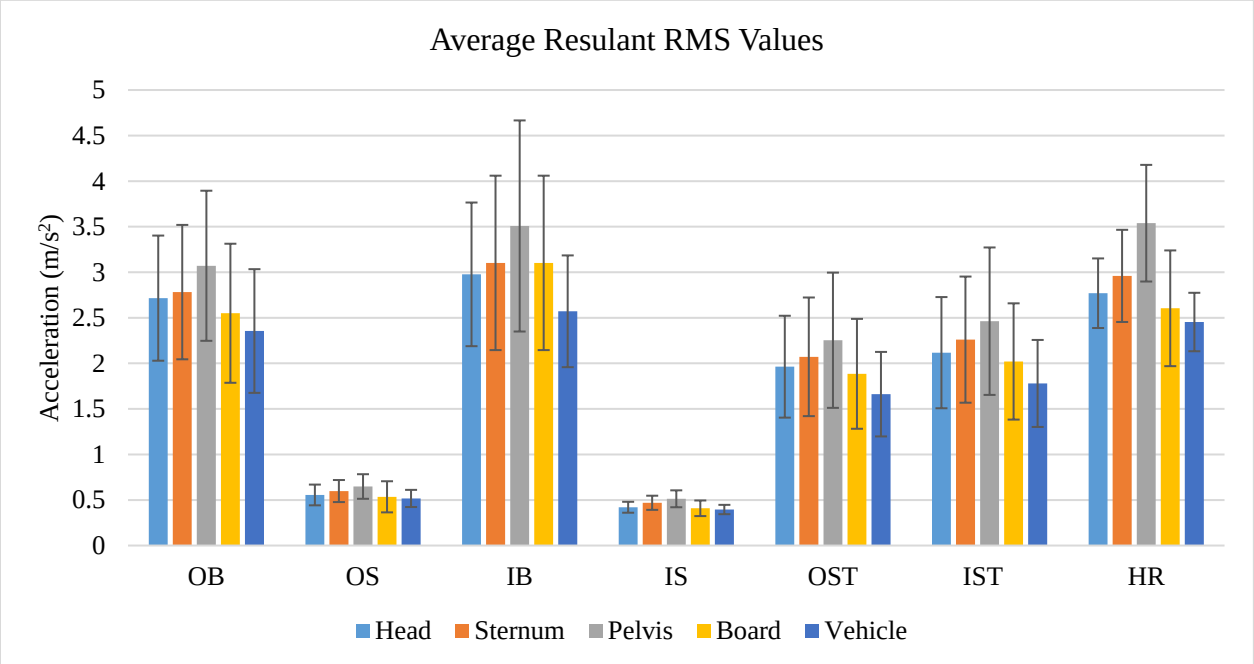

OB = Outside Bumpy, IB = Inside Bumpy, OS = Outside Smooth, IS = Inside Smooth,
OST = Outside Half Straddle, IST = Inside Half Straddle, HR = Half Round

Figure 12. Average resultant RMS values for the tracks for all of the subjects.

The standard deviations for the Bumpy, Straddle and Half Round conditions are higher compared to the Smooth conditions. Due to availability, the same exact vehicle was not used for all cohorts. Also, due to wear on the track from each pass, the track was resurfaced three

different times: between the first and second cohort, between the third and fourth cohort and again between the fourth and fifth cohort. Figure 13 shows the average resultant RMS values for the Outside Bumpy track for the different cohorts. An increase in resultant RMS can be seen each time after the track was repaired.

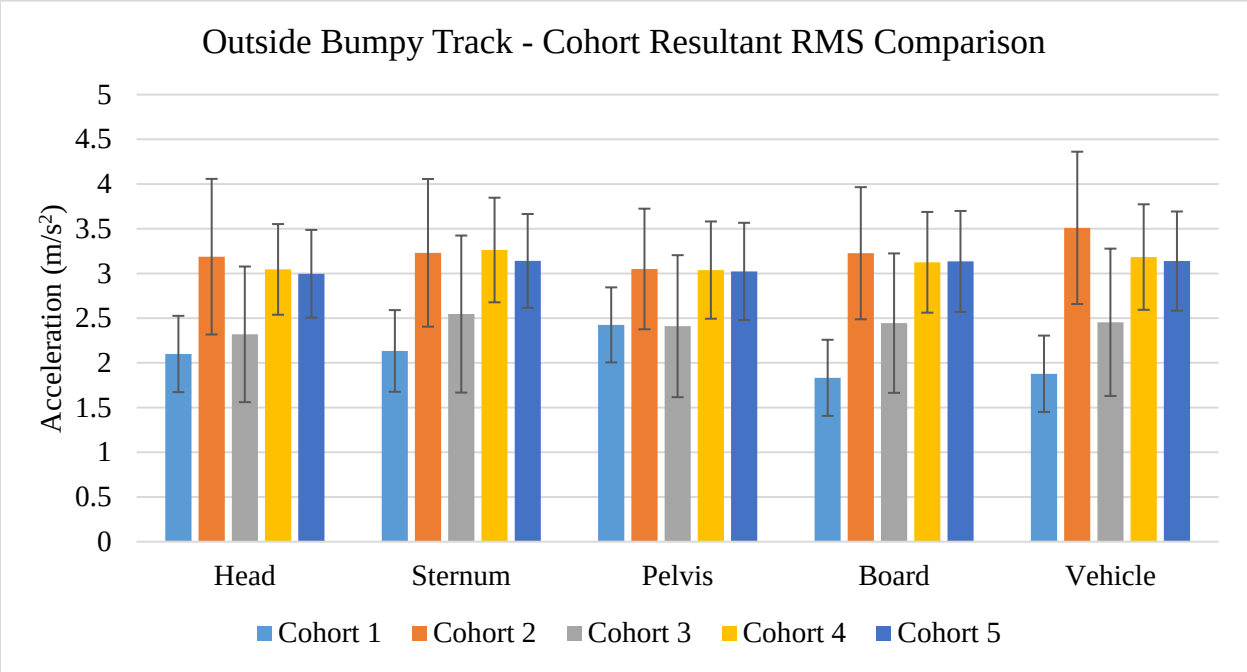

Figure 13. Outside Bumpy track cohort RMS comparison.

Figures 14 through 18 show the RMS accelerations for each sensor (head, scapula, pelvis, board, and vehicle). In each figure the *z*-axis shows the most motion. Similar to the previously shown Figure 12, the pelvis had the higher RMS values in the *z*-axis.

This space is intentionally blank.

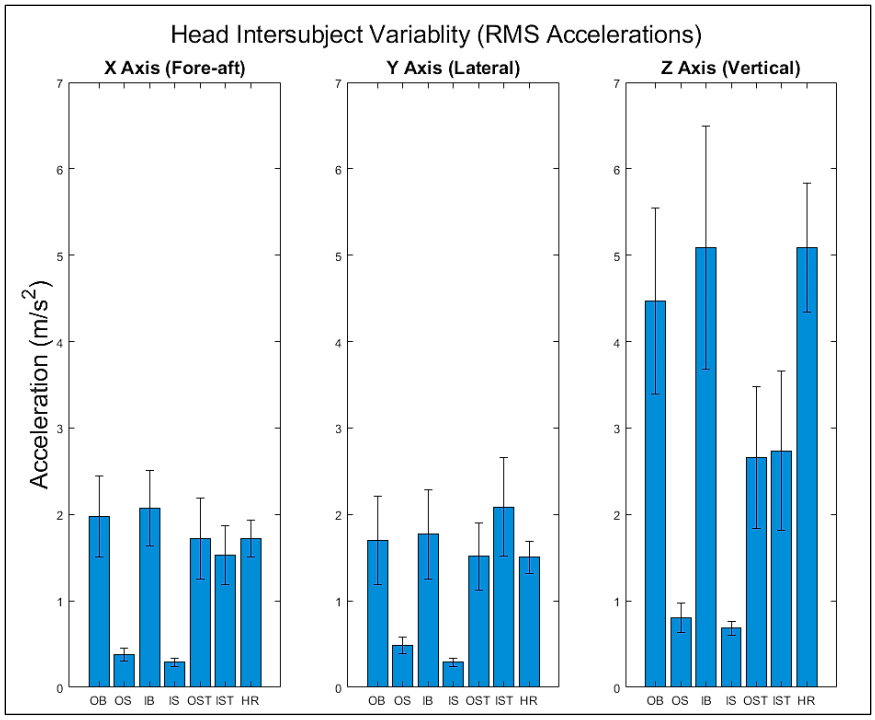

Figure 14. Head sensor average RMS accelerations for track segments (all cohorts).

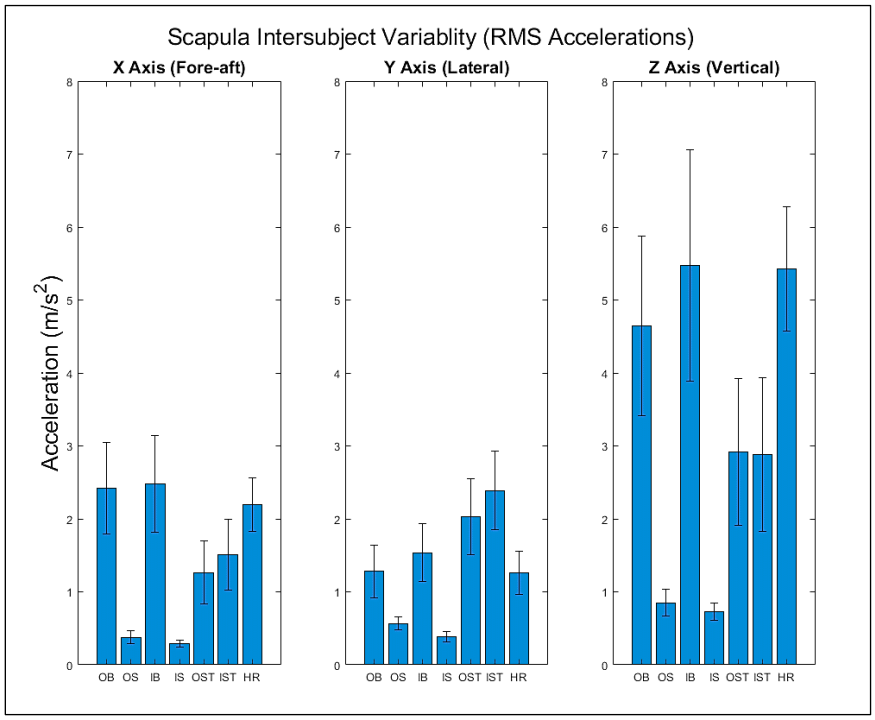

Figure 15. Scapula sensor average RMS accelerations for track segments (all cohorts).

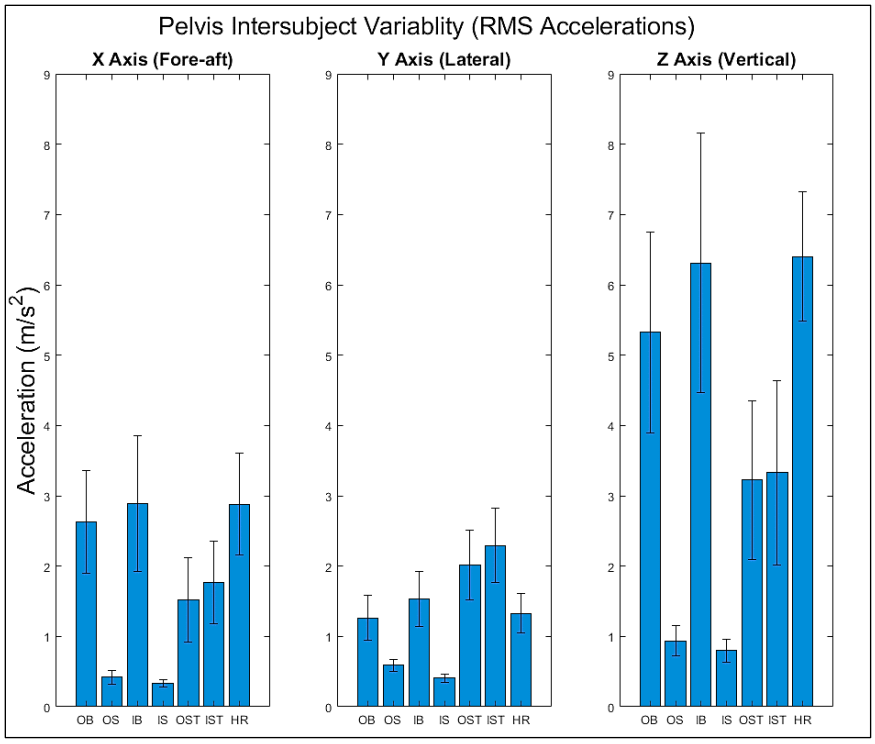

Figure 16. Pelvis sensor average RMS accelerations for track segments (all cohorts).

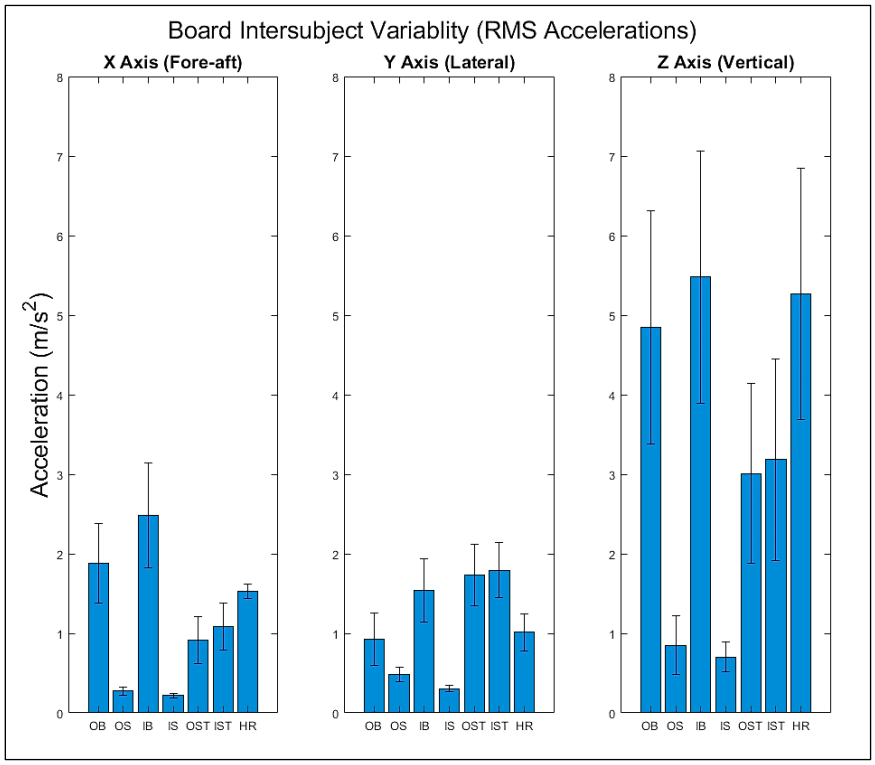

Figure 17. Board sensor average RMS accelerations for track segments (all cohorts).

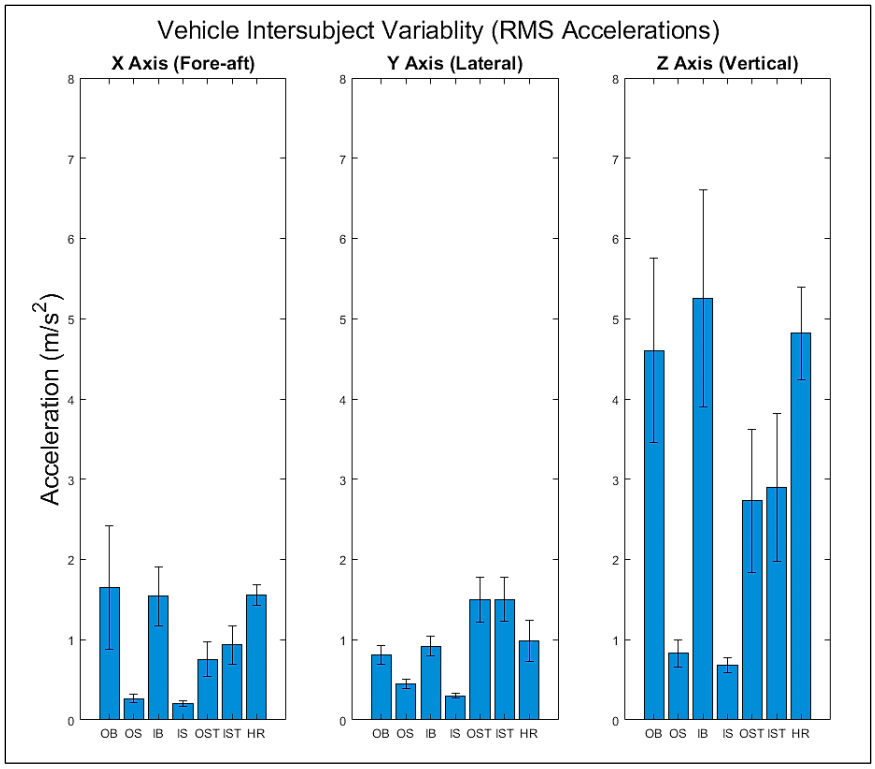

Figure 18. Vehicle sensor average RMS accelerations for track segments (all cohorts).

Power Spectral Density

The PSD functions were also calculated from the dataset using MATLAB®. When plotted across specific frequency bands, PSD describes the frequencies at which energy is present and at what levels. This is of particular interest when higher levels of energy are present in frequency bands that are known to have possible health effects on humans during whole-body vibration. The PSD was analyzed for each body segment, for each track. The mean of all subjects' PSD was used to identify where the most power was being transmitted to the subject. Figures 19 through 25 show the average PSD graphs for the sensors for each track condition. For each track and sensor axis the majority of the vibration occurred in the 1.5 to 3 Hz range, with peaks around 2 Hz. The pelvis (yellow line) experienced the highest amplitude of frequency for most of the tracks in the *x*- and *z*-axis. However, for the Outside Bumpy, Inside Bumpy, and Half Round tracks, the head showed the highest amplitude in the *y*-axis. Notably, the highest amplitude of energy is always present in the *z*-axis, for all body segment and tracks.

This space is intentionally blank.

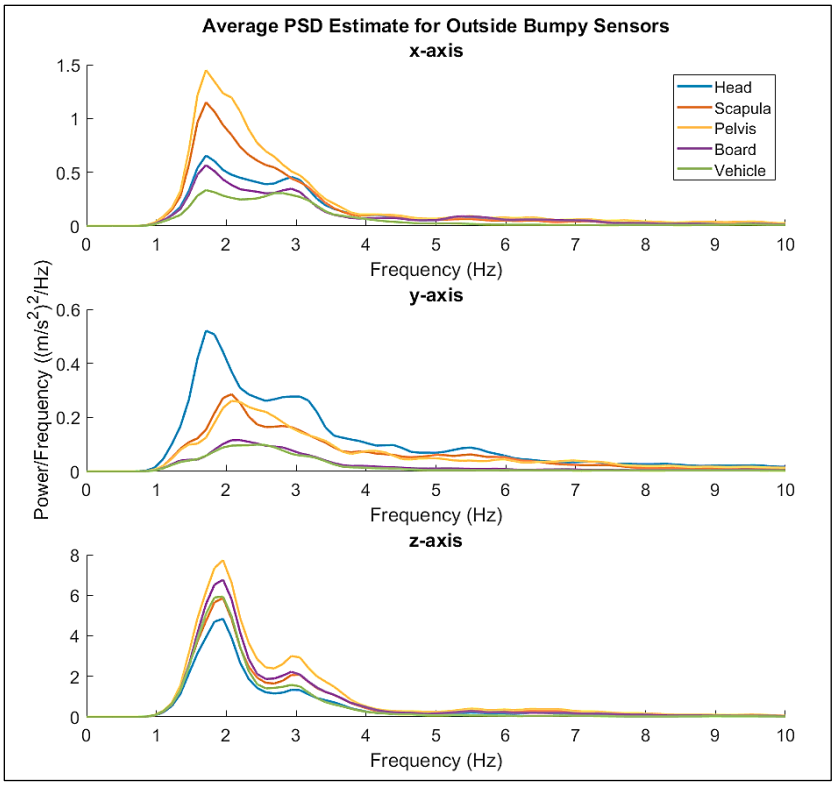

Figure 19. Average PSD estimate for each sensor for the Outside Bumpy section.

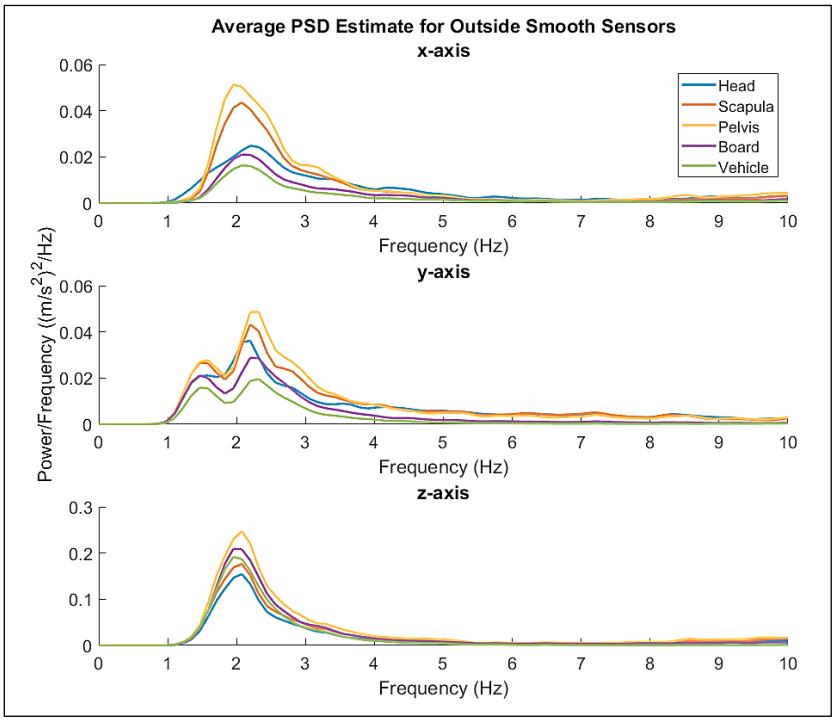

Figure 20. Average PSD estimate for each sensor for the Outside Smooth section.

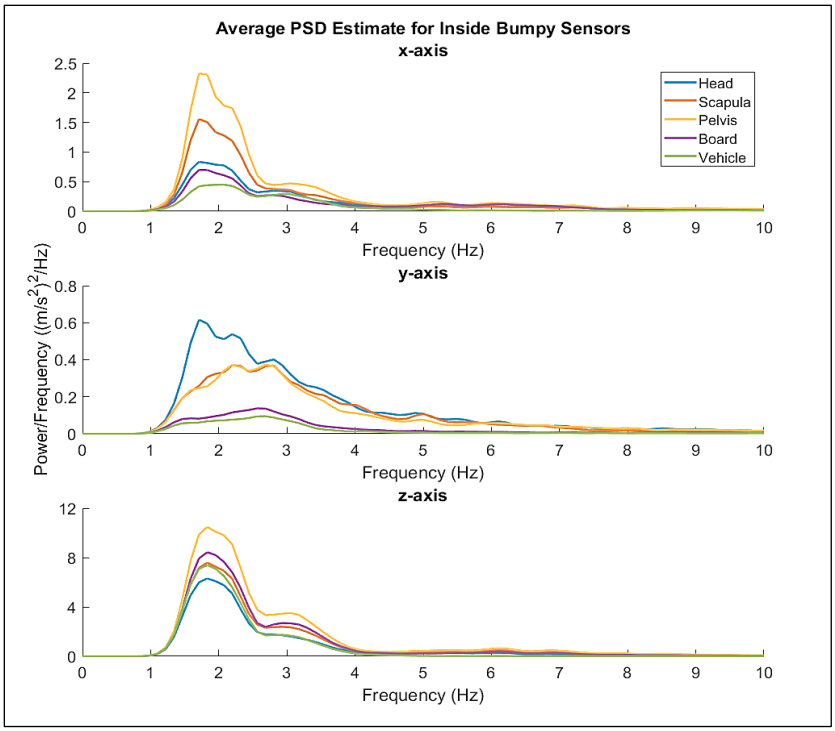

Figure 21. Average PSD estimate for each sensor for the Inside Bumpy section.

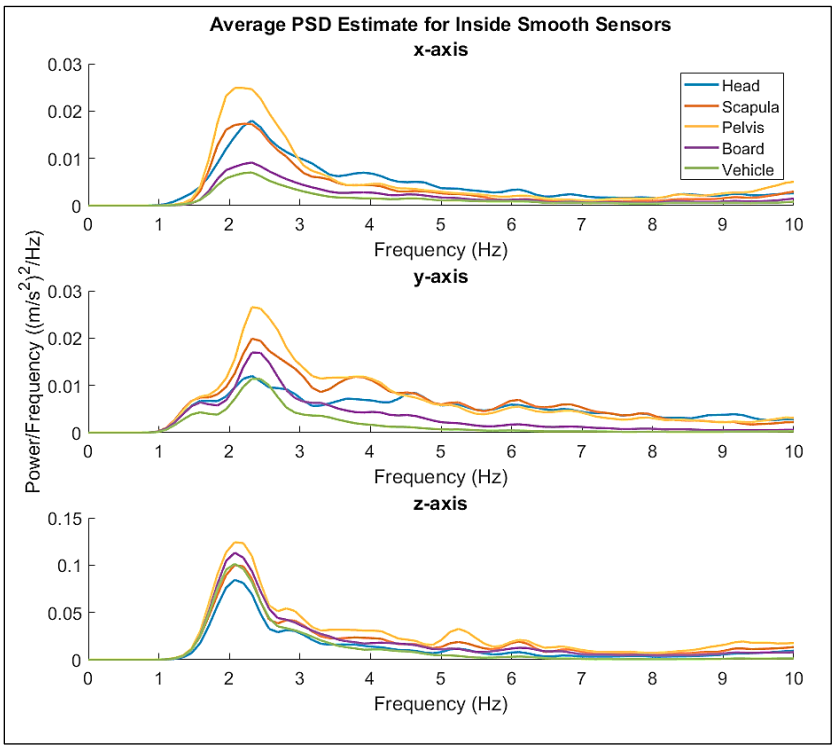

Figure 22. Average PSD estimate for each sensor for the Inside Smooth section.

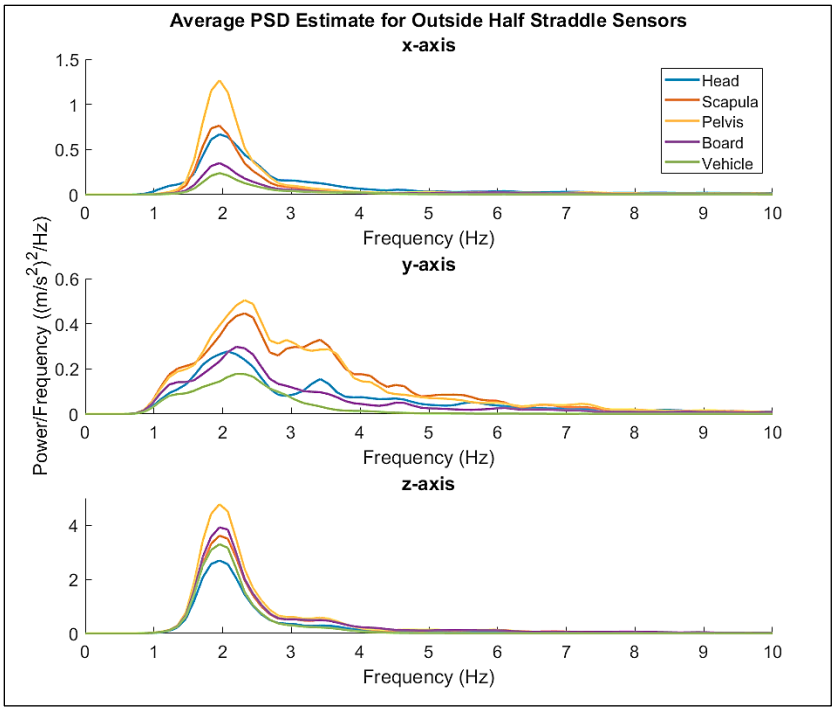

Figure 23. Average PSD estimate for each sensor for the Outside Half Straddle section.

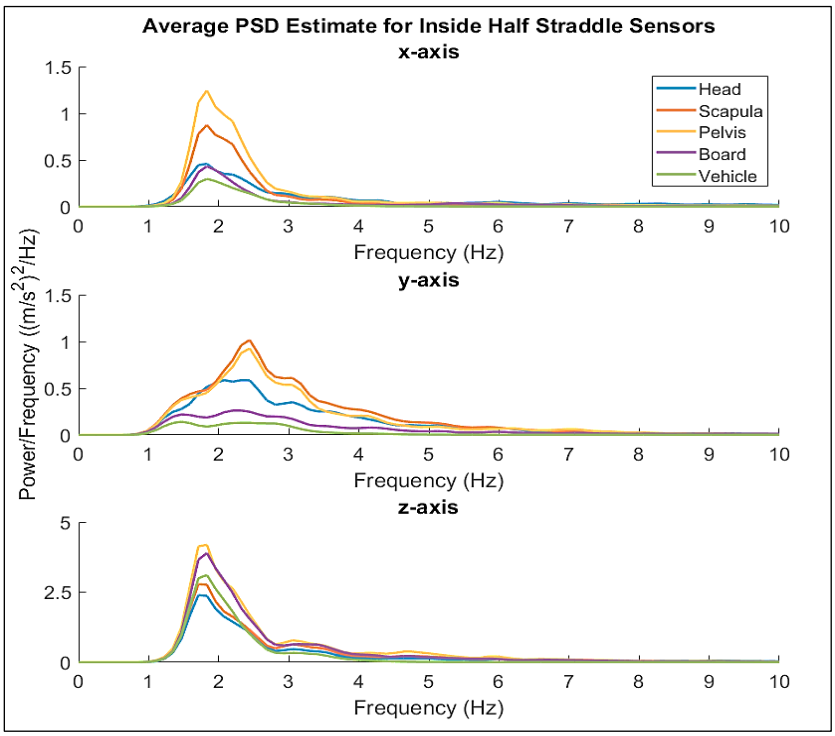

Figure 24. Average PSD estimate for each sensor for the Inside Half Straddle section.

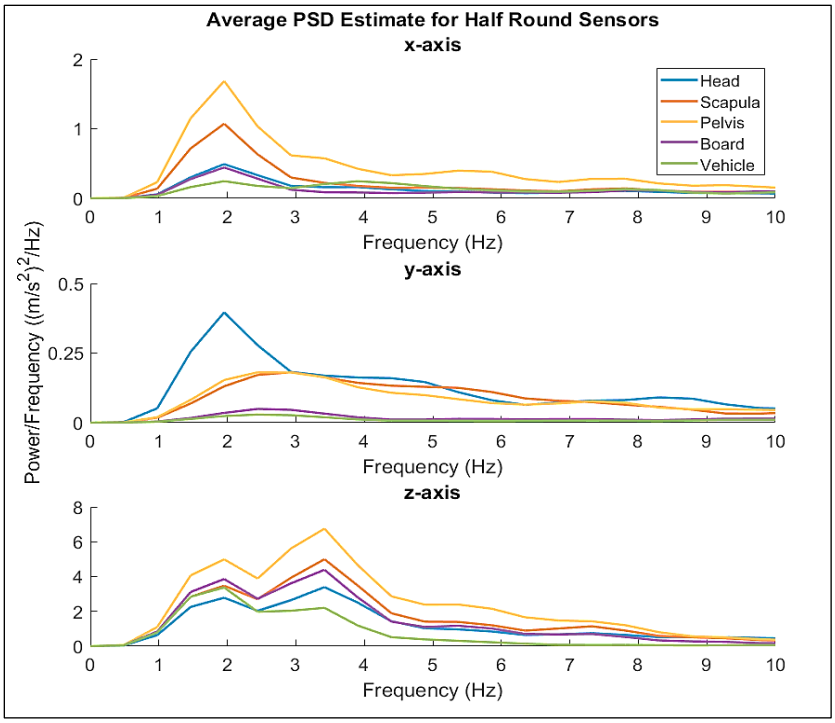

Figure 25. Average PSD estimate for each sensor for the Half Round.

Transmissibility

Transmissibility is the ratio of the output divided by the input. If the ratio is above 1.0 then there is amplification in the system. A transmissibility below 1.0 indicates that the output signal was attenuated, and if the ratio is equal to 1.0 then the output signal is equal to the input. Transmissibility has been used to characterize the human system as a single-output / single-input function or as a multiple-output / multiple-input function (Paddan & Griffin, 1998; DeShaw & Rahmatalla, 2014; Hinz, Menzel, Bluthner, & Seidel, 2010). For this analysis, the input acceleration was the litter berth of the vehicle. The output acceleration was the acceleration at each body segment of the subject (head, scapula, and pelvis). To find the transmissibility, the FFT of each segment was used to find the cross covariance, demonstrated in Table 8, which calculates the transmissibility in 3D space. The individual FFT graphs can be found in Appendix A. Figures 26 through 32 show the transmissibility cross-covariance for each of the track segments. The *x*-axis shows the frequencies and the *y*-axis shows transmissibility ratio.

This space is intentionally blank.

Table 8. Transmissibility Cross-Covariance Combinations

		Output Signal		
		Fore-aft Output (X)	**Lateral Output (Y)**	**Vertical Output (Z)**
Input Signal	**Fore-aft Input (X)**	Fore-aft Output ÷ Fore-aft Input (X/X)	Lateral Output ÷ Fore-aft Input (Y/X)	Vertical Output ÷ Fore-aft Input (Z/X)
	Lateral Input (Y)	Fore-aft Output ÷ Lateral Input (X/Y)	Lateral Output ÷ Lateral Input (Y/Y)	Vertical Output ÷ Lateral Input (Z/Y)
	Vertical Input (Z)	Fore-aft Output ÷ Vertical Input (X/Z)	Lateral Output ÷ Vertical Input (Y/Z)	Vertical Output ÷ Vertical Input (Z/Z)

/ = divided by

This space is intentionally blank.

The Outside Bumpy transmissibility graphs are shown in Figure 26, the pelvis sensor shown in black had the highest amplitude except lateral input, for which the head had the highest amplitude. The highest amplitudes were seen in the X/Y, Z/Y, and Z/X directions indicating that signal from the input (vehicle) was exacerbated at the output (through the animal subject).

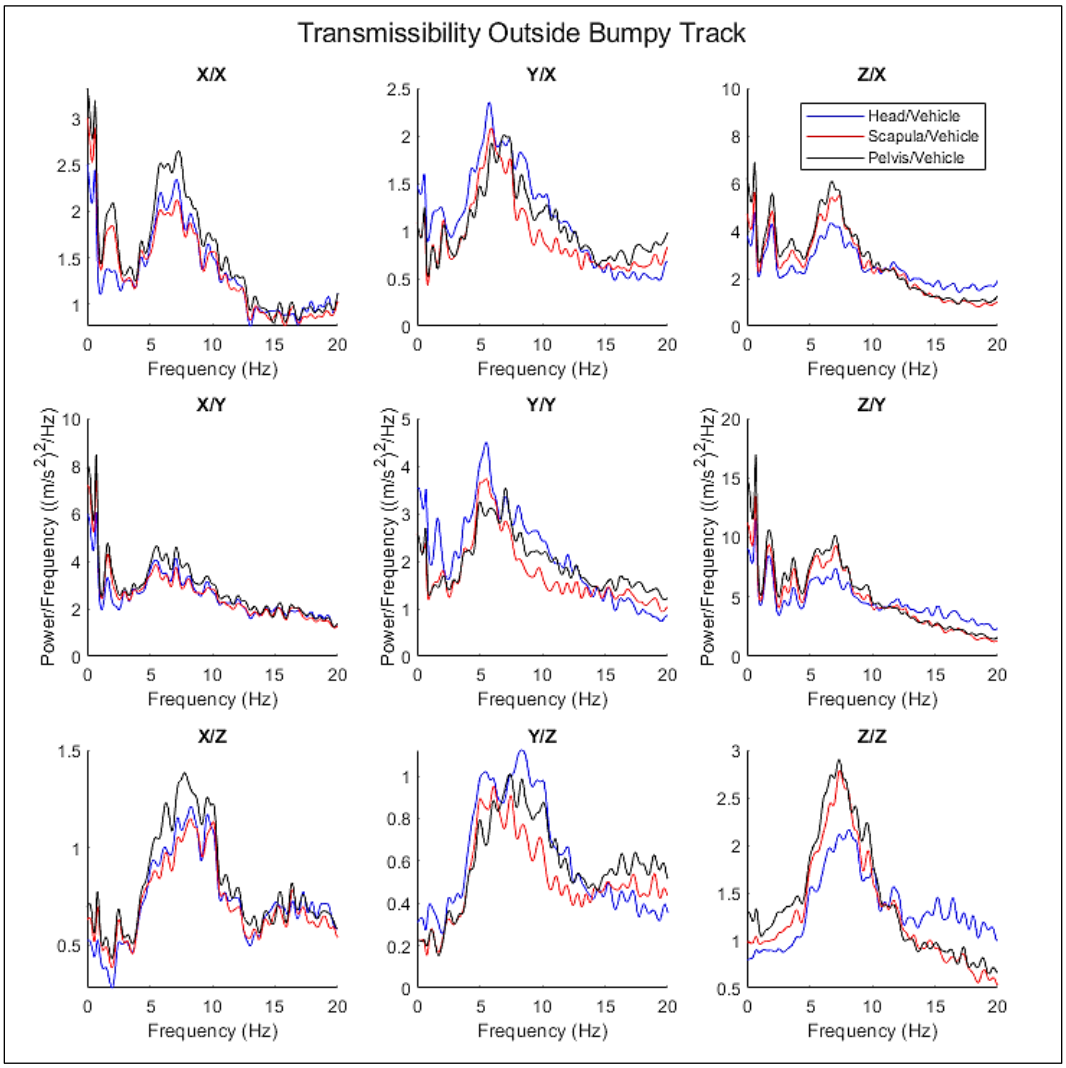

Figure 26. Transmissibility of the Outside Bumpy section.

This space is intentionally blank.

The Outside Smooth track transmissibility graphs are shown in Figure 27, for the vertical input divided by vertical output (X/X), the transmissibility values are below one for the head indicating that the input signal was mitigated. However, for lateral input and lateral output (Y/Y), the head had the highest transmissibility with the peak value almost double the peak value of the pelvis and scapula.

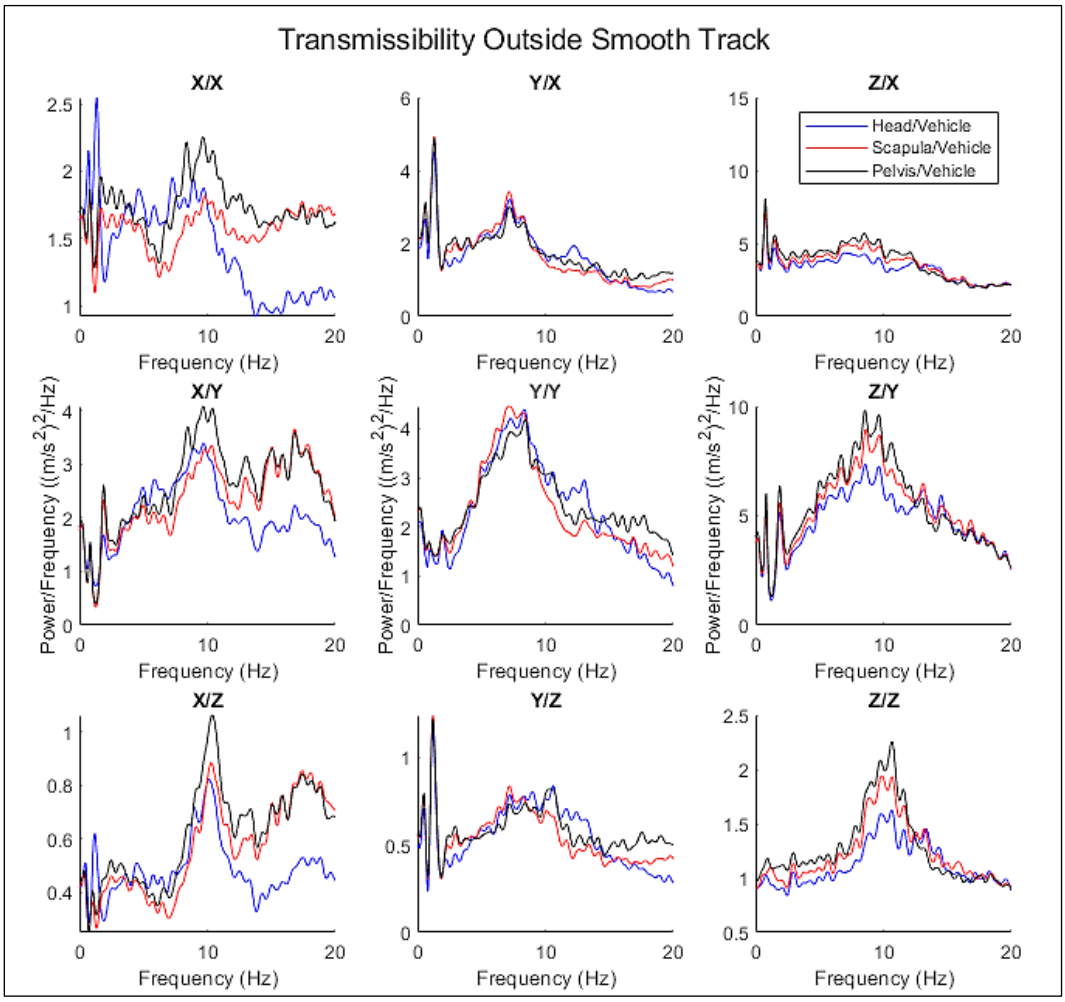

Figure 27. Transmissibility of the Outside Smooth section.

This space is intentionally blank.

The Inside Bumpy transmissibility graphs are shown in Figure 28, the results are similar to the Outside Bumpy the highest amplitudes were seen in the X/Y, Z/Y, and Z/X directions. The peaks in transmissibility can be seen over the range of 5 to 10 Hz for all graphs.

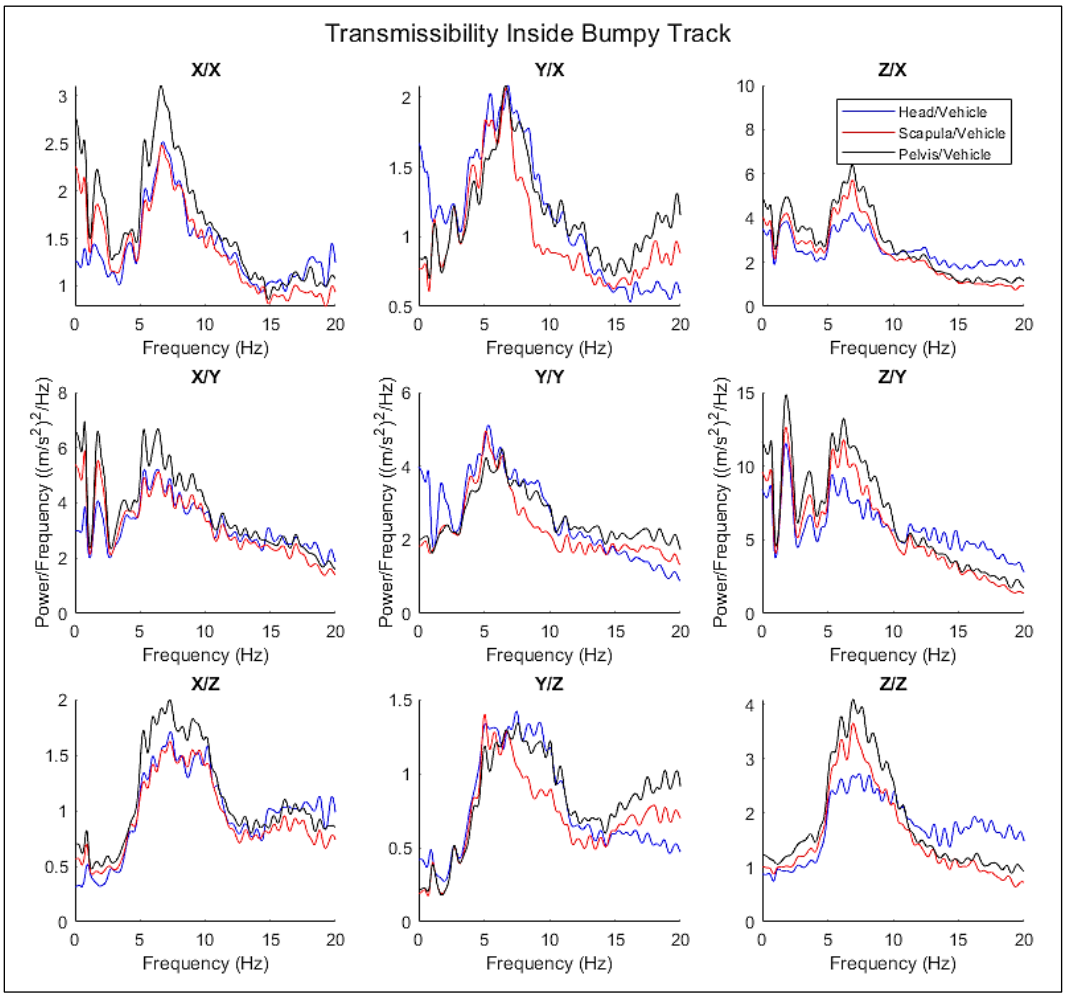

Figure 28. Transmissibility of the Inside Bumpy section.

This space is intentionally blank.

When comparing the Inside Smooth track transmissibility (Figure 27) to the Outside Smooth track transmissibility, there is less mitigation in X/X direction, but there is also less amplification in the Y/Y and Y/Z directions. Similar to the Outside Smooth track, Figure 24, there is a drop in transmissibility in the X/X direction for the Head/Vehicle after 10 Hz indicating that the output signal was mitigated.

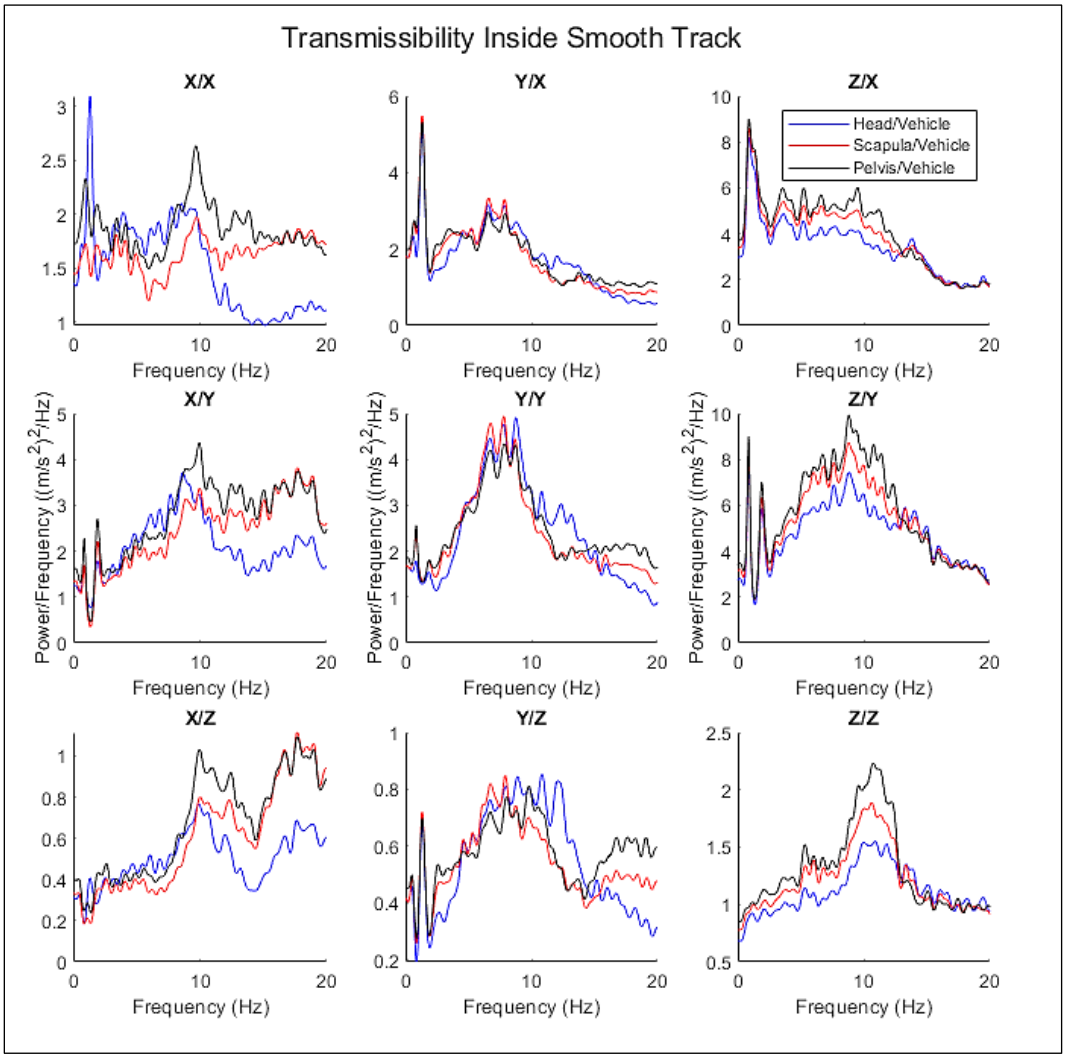

Figure 29. Transmissibility of the Inside Smooth section.

This space is intentionally blank.

The Outside Half Straddle transmissibility is seen in Figure 30, for the Outside Half Straddle section the left side of the vehicle (where the animal was located) was on the Outside Bumpy section and the right side of the vehicle was on the Outside Smooth section. Compared to the Outside Bumpy transmissibility there is an increase in transmissibility amplitudes for the lateral output (X/Y, Y/Y, and Z/Y) in the 5 to 10 Hz range indicating there was more lateral movement.

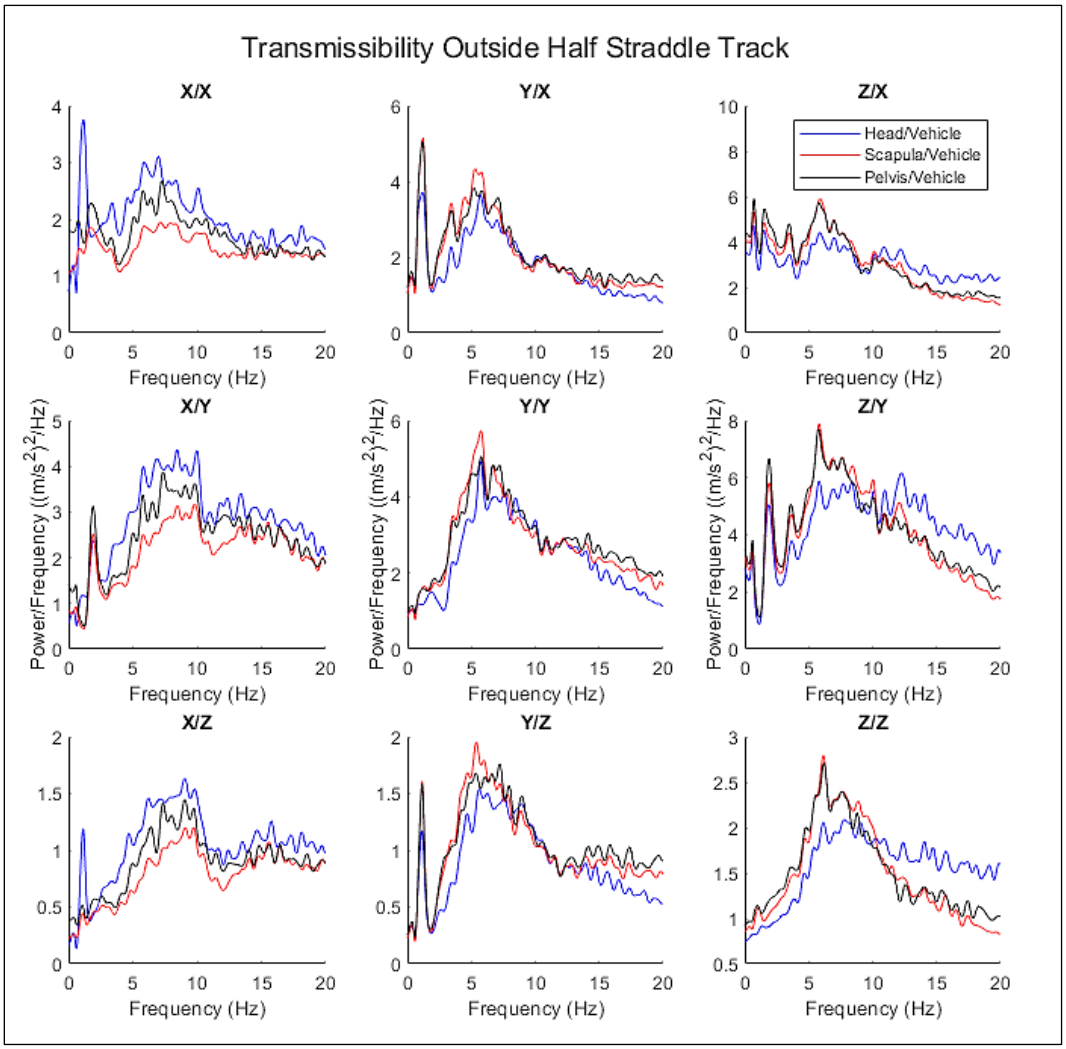

Figure 30. Transmissibility of the Outside Half Straddle section.

This space is intentionally blank.

For the Inside Half Straddle the left side of the vehicle (where the animal was located) was on the Inside Smooth section and the right side of the vehicle was on the Inside Bumpy section. Figure 29 shows the transmissibility ratios for the track segment. The peaks center around 6 Hz for all of the graphs.

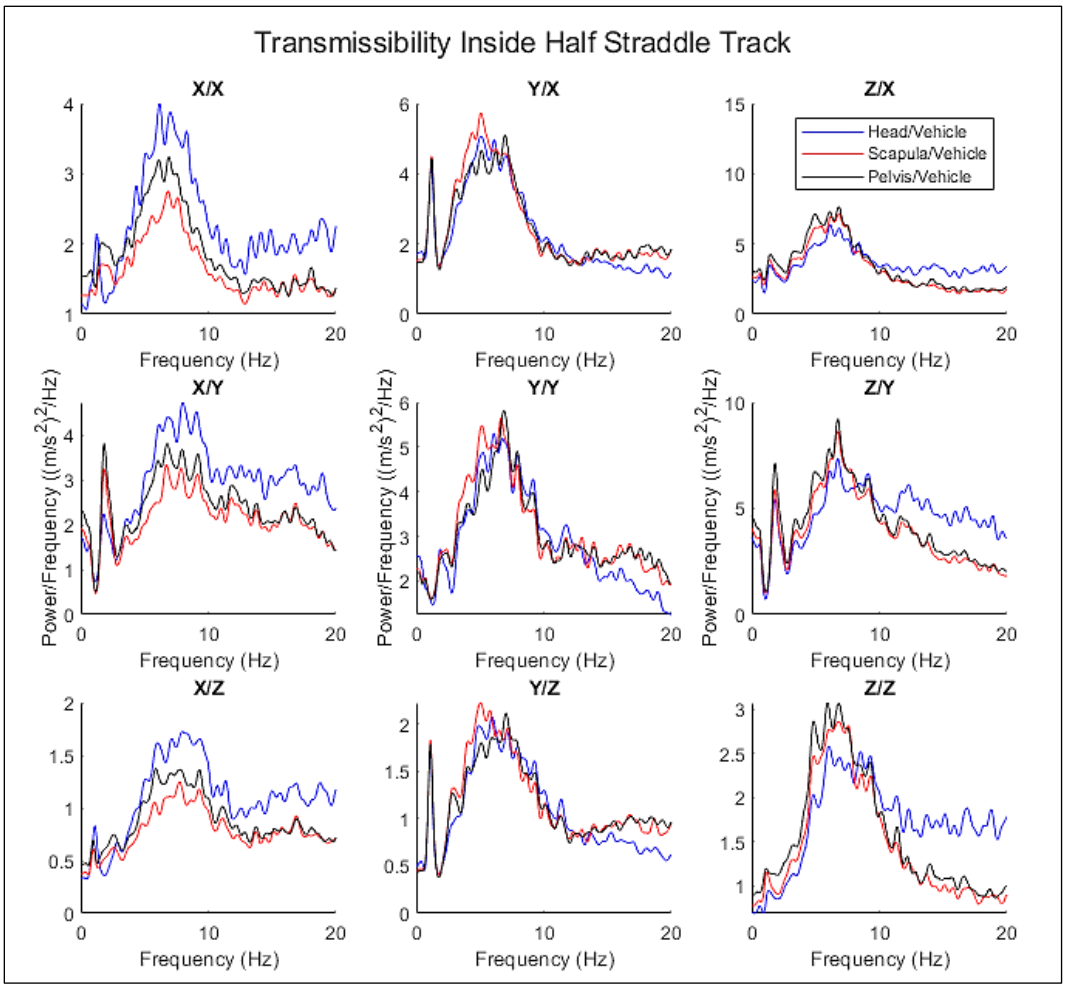

Figure 31. Transmissibility of the Inside Half Straddle section.

For the Half Round, the transmissibility cross-covariance are shown in Figure 30. The Half Round analysis showed large spikes in the transmissibility in the lower frequencies (0 to 2 Hz) along with high amplitudes in the 5 to 10 Hz range. The Z/X and Z/Y graphs show peaks of 30 and 15 respectively indicating a high level of increase in the fore-aft and lateral input signals when compared to the vertical output.

This space is intentionally blank.

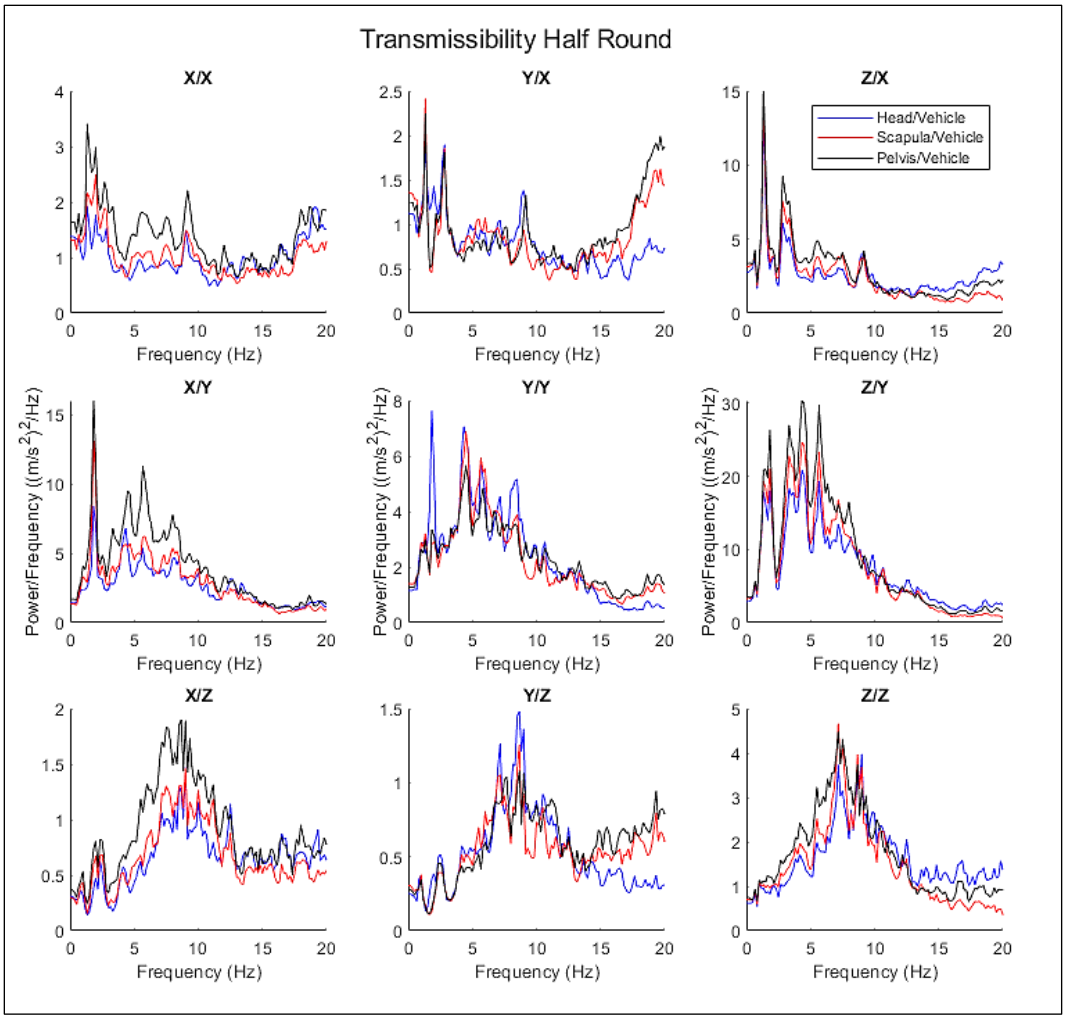

Figure 32. Transmissibility of the Half Round.

Discussion

From the RMS analysis it was found that the resultant RMS calculated from the data from the pelvis sensor was 12 to 16% higher than the other sensors for all of the tracks. A possible reason is that the pelvis of the animal was positioned in the middle of the backboard and litter, which was not strapped down to the vehicle litter berth in the same manner as the ends of the litter. This allowed flexing of the litter mesh and poles, and subsequently the backboard at this area, exacerbating the energy input to the pelvis. There were differences between cohorts in resultant RMS, dependent on the track wear and vehicle suspension. The same vehicle was not used for each cohort, and the track was resurfaced between some of the cohorts. These factors contributed to the high standard deviations between the cohorts.

The PSD analysis also showed that in most cases the pelvis experienced the most power amplitude for all tracks and all axes. Some of the exceptions to this were seen in the y-axis on the Inside Bumpy, Outside Bumpy, and Half Round sections, where the head showed the greatest power amplitude. This could be due to the shape and taper of the animal subject's head, which

the head blocks were not designed for, and so may have allowed a small amount of lateral movement to occur on exceptionally rough terrain. The pelvis was positioned over the middle of the litter which is where the most flexion in the litter occurs during hard bumps. The gross movement of the litter during the bumpy track passes exacerbated the pelvis movement. For this study, the main vehicle input vibration was centered between 1.5 to 3 Hz as seen by the PSD analysis. The resonance frequencies of the decontamination litter and human body are within the 4 to 6 Hz range (Rahmatalla et al., 2020; Wanner, Mayer, Kinsler, & Helgeson, 2017). It is not clear if the vehicle input vibration frequencies are close enough to those resonance frequencies to cause exacerbation of the input energy.

The transmissibility calculations are characterized by peaks around 5 to 10 Hz, which is likely linked to the resonance frequency of the vibration response of the litter. The transmissibility is a useful measure of the characteristics of a system under vibration because it defines how the vibrations are altered while traveling through a material or structure, either attenuating, amplifying, or shifting energy to different frequencies. However, the metric gives less accurate results when a very narrow band of input vibration is present. That being said, one of the notable features in the transmissibility graphs is that nearly all values are above 1, meaning that the energy input from the vehicle was being exacerbated for nearly all input-output combinations, with some exceptions on the smooth tracks. In addition, the graphs in the *z*-input column show much higher values than the corresponding graphs in the *x*- and *y*-input columns. This means that the majority of the stress placed on the subject during transport seems to come from the vertical energy input from the vehicle. Since the *z*-axis input from the vehicle was not trivial, the ratio of the output to input being so large is especially concerning.

Conclusions

This study identified the transportation stresses the injured swine model experienced during transport. Considering the body movement of injured patients during transport when designing litters, immobilization systems, medical interiors, and transport vehicles is important to improving patient outcomes. Technologies like vibration mitigation layers can be developed and tested using similar methods as described in this report.

Some possible steps that could be taken to make the results more accurately repeatable would include the procurement of a single vehicle to use for all testing, and resurfacing of the test track before all cohorts to ensure it is in comparable condition during testing.

The transmissibility demonstrated that all axes, especially the *z*-input axis, exacerbate the input energy from the vehicle. Vibration mitigation may play an important role in reducing subject morbidity and mortality during transport.

Further comparisons need to be completed to determine if the injured swine model results can be translated to human patients. A complementary study was completed on healthy human subjects, who were transported on the same track, with a similar sensor setup. Further analyses will be forthcoming examining the extrapolation from the injured animal model response and healthy human response to the injured human biodynamic response.

References

Cullen, D.K., Harris, J.P., Browne, K.D., Wolf, J.A., Duda, J.E., Meaney, D.F., Margulies, S.S., and Smith, D.H. (2016). *A Porcine Model of Traumatic Brain Injury via Head Rotational Acceleration.* Methods Mol Biol 1462, 289-324.

DeShaw, J., & Rahmatalla, S. (2014). *Predictive discomfort in single-and combined-axis whole-body vibration considering different seated postures.* Human Factors: The Journal of the Human Factors and Ergonomics Society, 56(5), 850-863.

Hinz, B., Menzel, G., Bluthner, R., & Seidel, H. (2010). Seat-to-head transfer function of seated men--determination with single and three axis excitations at different magnitudes. Industrial Health. 48(5), 565-583.

Mayer, A.R. (2019). *Increased Survival Rate Following Hemorraghic Shock and Traumatic Brain Injury in Austere Environments.* U.S. Army Medical Research and Materiel Command Annual Report.

Mayer, A.R., Dodd, A.B, Vermillion, M.S., Stephenson, D.D., Chaudry, I.H., Bragin, D.E., Gigliotti, A.P., Dodd, R.J., Wasserott, B.C., Shukla, P., Kinsler, R., & Alonzo, S.M. (2019). *A systematic review of large animal models of combined traumatic brain injury and hemorrhagic shock.* Neuroscience & Behavioral Reviews, 104:160-177.

Mayer, A.R., Dodd, A.B., Ling, J.M., Stephenson, D.D., Rannou-Latella, J.G., Vermillion, M.S., Mehos, C.J., Johnson, V.E., Gigliotti, A.P., Dodd, R.J., Chaudry, I.H., Meier, T.M., Smith, D.H., Bragin, D.E., Lai, C., Wagner, C.L., Guedes, V.A., Gill, J.M., & Kinsler, R. (2020). *Survival rates and biomarkers in a large animal model of traumatic brain injury combined with two different levels of blood loss.* Shock Society Journal.

Paddan, G.S., &Griffin, M.J. (1998). *A Review of the Transmission of Translational Seat Vibration to the Head.* Journal of Sound and Vibration, 215, 863-882.

Rahmatalla, S., Kinsler, R., Qiao, G., DeShaw, J., and Mayer, A. (2020). *Effect of gender, stature, and body mass on immobilized supine human response during en route care transport.* J Low Freq Noise V A.

Wanner, I., Mayer, A., Kinsler, R., and Helgeson, M. (2017). *Improved Field Management and Safe Ground Transport of Patients with Head and Spine Injuries.* Final Annual Report.

Appendix A. Fast Fourier Transform Graphs

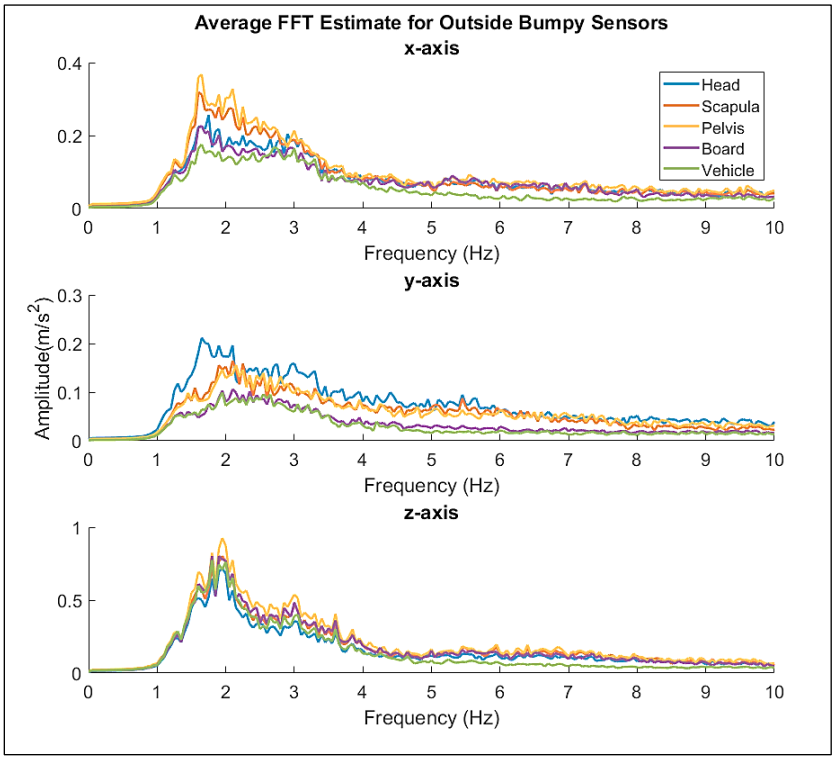

Figure A1. Average FFT estimate for all sensors for the Outside Bumpy section.

This space is intentionally blank.

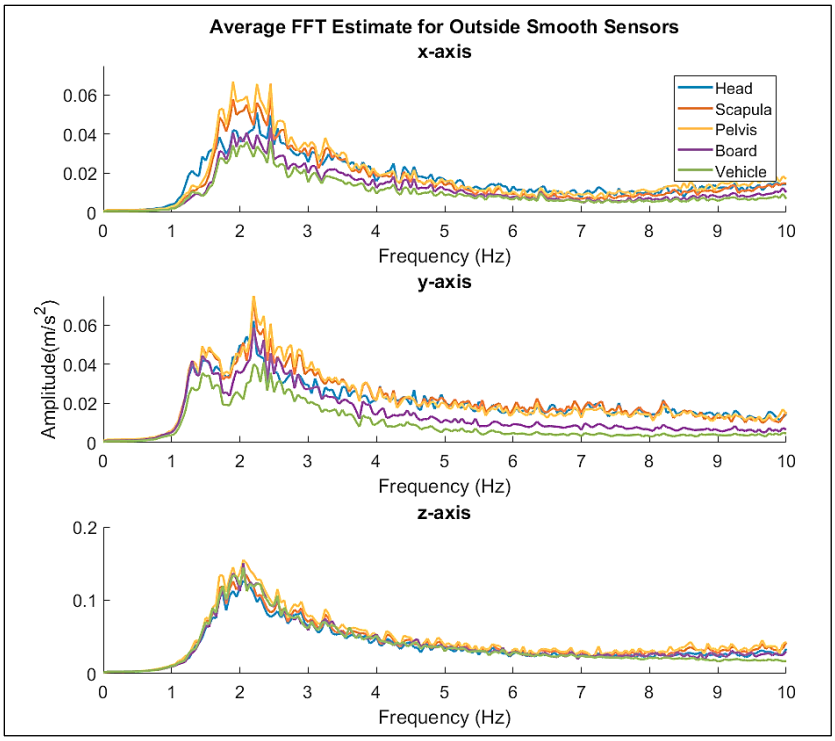

Figure A2. Average FFT estimate for all sensors for the Outside Smooth section.

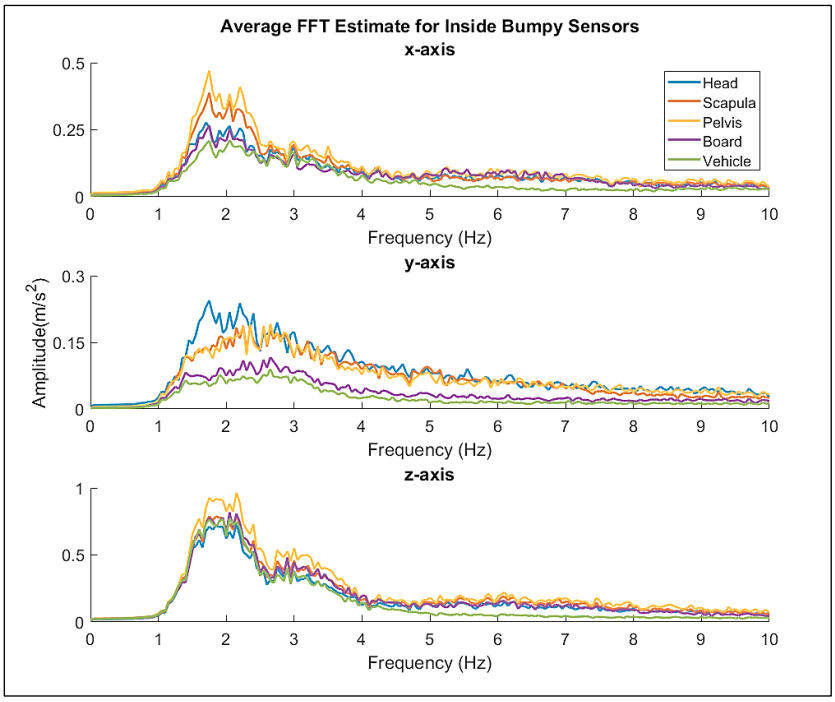

Figure A3. Average FFT estimate for all sensors for the Inside Bumpy section.

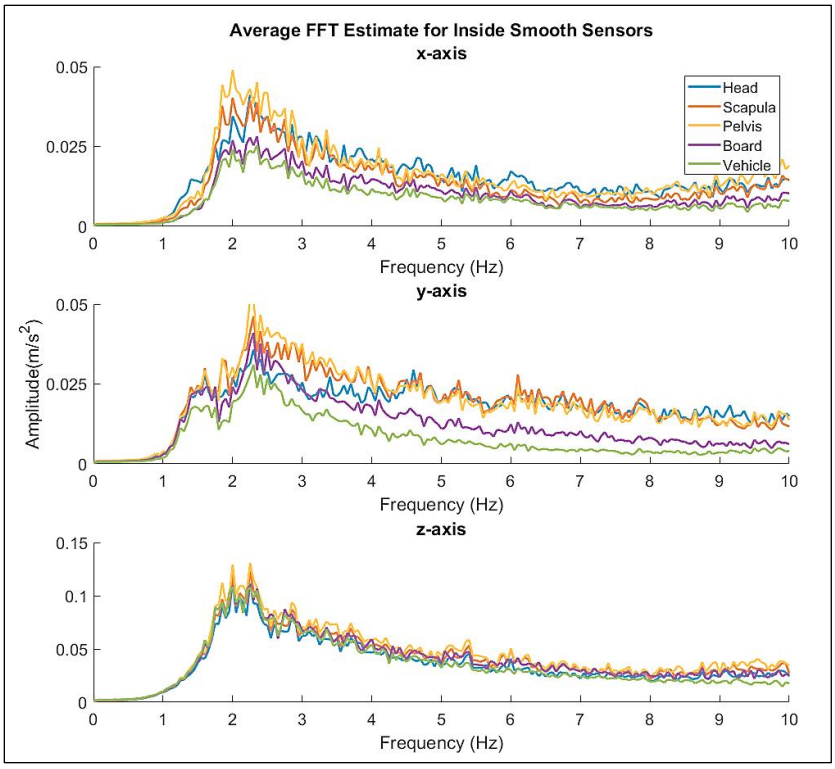

Figure A4. Average FFT estimate for all sensors for the Inside Smooth section.

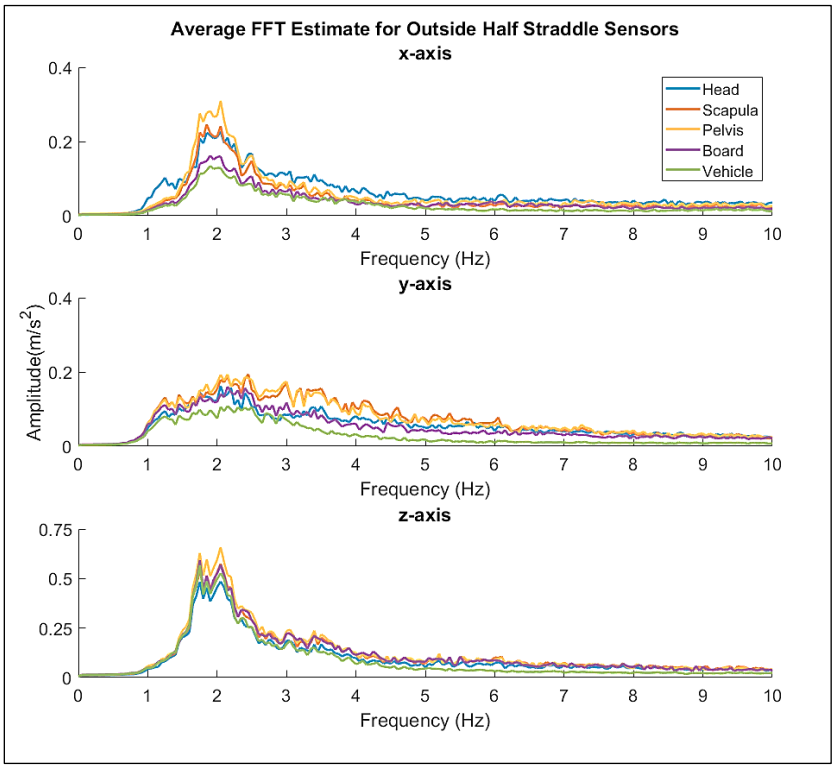

Figure A5. Average FFT estimate for all sensors for the Outside Half Straddle section.

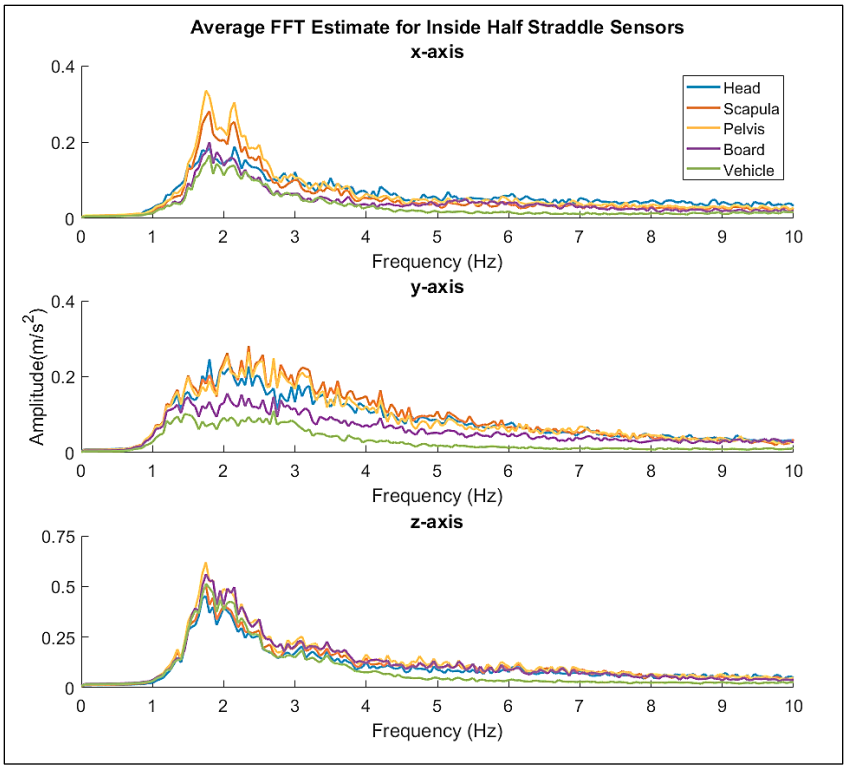

Figure A6. Average FFT estimate for all sensors for the Inside Half Straddle section.

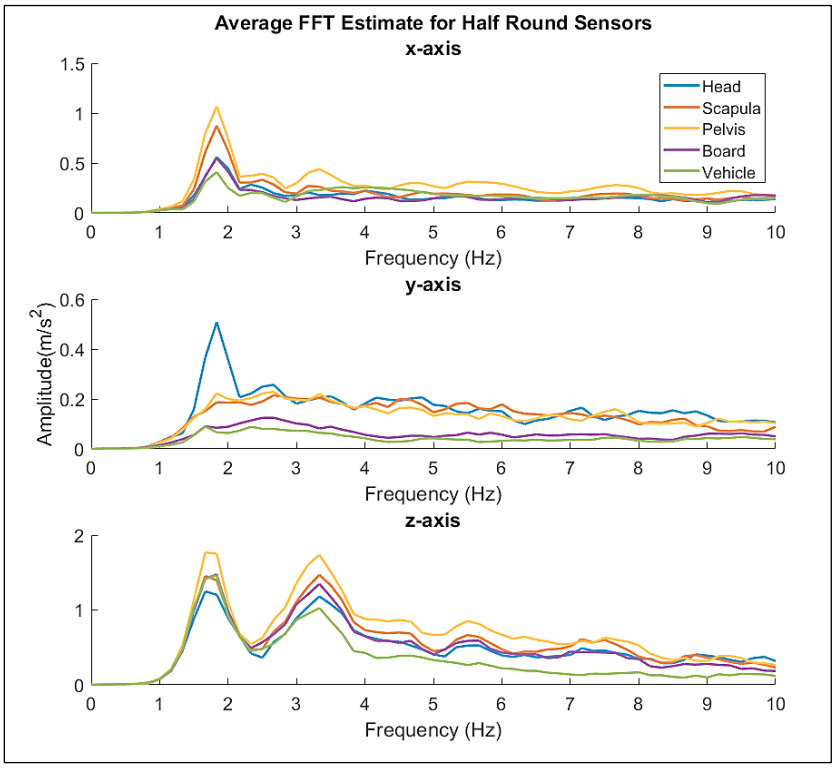

Figure A7. Average FFT estimate for all sensors for the Half Round.

Appendix B. Acronym List

6DOF – 6 Degrees of Freedom

DAQ – data acquisition

DTIC – Defense Technical Information Center

FFT – Fast Fourier Transform

HS – hemorrhagic shock

Hz – Hertz

LBRI – Lovelace Biomedical Research Institute

mph – miles per hour

PFC – prolonged field care

PSD – Power Spectral Density

RMS – root mean square

TBI – traumatic brain injury

USAARL – United States Army Aeromedical Research Laboratory

U.S. Army Aeromedical Research Laboratory
Fort Rucker, Alabama

All of USAARL's science and technical information documents are available for download from the Defense Technical Information Center.

https://discover.dtic.mil/results/?q=USAARL

Army Futures Command
U.S. Army Medical Research and Development Command